A COMPREHENSIVE STUDY OF THE EFFECTS OF EEG ELECTRODE ARRAYS ON MRI SIGNAL-TO-NOISE AT 3T

by

AMAN ISH GOYAL

Presented to the Faculty of the Graduate School of

The University of Texas at Arlington in Partial Fulfillment

of the Requirements

for the Degree of

MASTER OF SCIENCE IN BIOMEDICAL ENGINEERING

THE UNIVERSITY OF TEXAS AT ARLINGTON

December 2006

Copyright © by Aman Ish Goyal 2006

All Rights Reserved

ACKNOWLEDGEMENTS

I thank my thesis supervisor, Dr. Richard Briggs from the deepest recesses of my heart. He was very busy the past few months, but he still found time as well as energy to guide me during the course of my thesis research project. Without his valuable input, guidance and encouragement I would have been lost. I consider myself blessed to have him as my teacher.

I also thank Dr. Hanli Liu and Dr. Roderick McColl for graciously agreeing to be on my thesis committee and for their insightful inputs about my thesis.

Dr. Subhendra Sarkar always made sure that I did the things right way during my experiments at the 3T scanner. His suggestions have been extremely useful.

My colleagues in the lab, Audrey Chang and Xiufeng Li, have always had words of encouragement for me. I thank Cynthia Johnson, our administrative secretary, for helping me on the day of my thesis defense presentation.

I am also thankful to Curtis Ponton, Chief Scientific Officer, Compumedics-Neuroscan, for providing us with a 32-channel EEG electrode cap at a very short notice and to Dr. Evelyn Babcock for letting me use the GE phantom for so long.

Lastly and most importantly, I wish to thank my parents and my younger brother. They have always been there for me even though I haven't been there for them. To them I dedicate this thesis.

November 21, 2006

ABSTRACT

A COMPREHENSIVE STUDY OF THE EFFECTS

OF EEG ELECTRODE ARRAYS ON

MRI SIGNAL-TO-NOISE AT 3T

Publication No. _____

Aman I Goyal, MS

The University of Texas at Arlington, 2006

Supervising Professor: Dr. Richard W. Briggs

Simultaneous EEG-fMRI offers much potential for gaining complementary, noninvasive information about brain function. While much effort has been devoted to the compelling problem of removing ballistocardiogram and gradient artifacts from the EEG waveforms, less attention has been paid to the impact that increasing density of electrode arrays has on the MR images. Initial work reporting the effects of EEG caps and electrodes on the MR image has been site specific, using customized EEG equipment that those research groups built in-house. Therefore these results are hard to generalize to other laboratory environments. A monotonic decrease in SNR of the images has been reported upon increasing the density of the EEG electrode array. The

aim of this study was to do preliminary measurements to compare effects on MRI SNR for 32, 64 and 128 electrodes in a Compumedics-Neuroscan MagLink EEG system, using copper versus carbon - fiber cables and transmit-receive circularly polarized head coil versus 12-channel receive-only array head coil. It was found by this study that the drop in the SNR of MR images with an increase in the EEG array density is not so straight forward. It was also understood by pursuing this project that different head coils interact differently with the EEG electrode arrays.

TABLE OF CONTENTS

LIST OF ILLUSTRATIONS

LIST OF TABLES

CHAPTER 1

INTRODUCTION

As researchers delve deeper into the functioning and functional organization of human brain, the choice of technique itself has become an important question. Many imaging modalities such as PET (Positron Emission Tomography), SPECT (Single Photon Emission Computed Tomography), BOLD fMRI (Blood Oxygen Level Dependent functional MRI), ASL fMRI (Arterial Spin Labeling fMRI), NIRS (Near Infra-red Spectroscopy), MEG (Magnetoencephalography) and EEG (Electroencephalography) have been used to image human brain. Although all of them aim to explain brain function, each one of them is based on a different physiological measure and has varied technical implementation. A very brief description of these techniques and their relative advantages and disadvantages is presented in the following few paragraphs.

1.1 Brief Description of Functional Brain Imaging Techniques

PET (Positron Emission Tomography) and SPECT (Single Photon Emission Computed Tomography) are based on the use of radioactive nuclei, which are injected into the blood stream as radiotracers. While PET registers the photons emitted from the

annihilation of a positron (released by the radionuclide – O-15, F-18 etc.) and an electron, the radiotracers used in SPECT (e.g. Xe-133) emit gamma rays. The emissions (photons in PET and gamma rays in SPECT) are detected by a set of detectors and are reconstructed into images based on the back projection technique. While PET can be used to map neurotransmitters, SPECT is most commonly used to measure regional cerebral blood flow (rCBF). The major disadvantages of a PET system are the prohibitively huge cost of the instrument and of generating radioisotopes and its use of radioactive nuclei. Although a SPECT system is cheaper than a PET system, it offers limited spatial and temporal resolution.

BOLD fMRI (Blood Oxygen Level Dependent functional MRI) and ASL fMRI (Arterial Spin Labeled fMRI) of the brain are two MRI-based functional brain imaging techniques. BOLD fMRI signal is an indirect measure of brain function. The difference in susceptibility of oxygenated and deoxygenated blood is the basis of this measure. On the other hand, ASL lets us measure the absolute cerebral blood flow by labeling the arterial blood non-invasively. While BOLD already has been used extensively for functional brain imaging studies, ASL is still in nascent stages of its development. Although an MRI system is costly, it offers very fine spatial resolution (1-5 mm).

NIRS (Near Infra-red Spectroscopy) is probably the least invasive of all the imaging techniques, as it is based on light in the visible band of the electromagnetic spectrum and there is no high-energy radiation or high magnetic field used. Light, as it travels through the tissue, is attenuated differently by different tissue. On the other end, a sensor detects the transmitted light and an image of the tissue that it just traversed is

generated based on the amount of light absorbed at specific wavelengths. Low cost and non-invasiveness are its biggest advantages. NIRS's application to brain imaging is beginning to be pursued with great interest.

EEG (electroencephalography) and MEG (magnetoencephalography) measure the electrical signals from the brain. Accurate localization within the brain of the source(s) of these signals from surface measurements requires an inverse solution for the electromagnetic field equations, which is difficult. The brain emits electrical signals at different frequencies in different states. EEG is used to record this electrical activity. MEG measures the associated magnetic fields. The primary disadvantage of both of these modalities is poor spatial localization capability, especially in deep brain structures. But EEG and MEG offer the huge advantage of very fine temporal resolution (millisecond range) over all other imaging modalities.

Combination of two or more of the above-mentioned techniques can offer a great insight into the working of human brain. Simultaneous EEG – fMRI is one such step in this direction.

1.2 Simultaneous EEG – fMRI

Simultaneous EEG and fMRI of the brain is increasingly becoming the technique of choice for the researchers who are trying to explain the complexities of brain function. While EEG signals relate directly to the electrical activity of neuronal firing, BOLD fMRI reports signal changes due to local changes in blood oxygenation,

flow, and volume, subsequent to the metabolism involved with neuronal activity. Though the two techniques of EEG and fMRI evolved separately, studies have shown that the two seem to complement each other well [1, 2]. EEG provides millisecond time resolution of the neuronal activity, but poor spatial localization of that activity (ca. 10 cm), while fMRI has good spatial resolution (1-5 mm), but poorer temporal resolution (ca. 0.1-1 s).

In simultaneous EEG – fMRI, EEG recordings are obtained while the subject is inside an MRI scanner for a brain scan. Bringing two techniques together and using them in conjunction with each other has been fraught with technical challenges. The challenges that arise from trying to acquire EEG and fMRI simultaneously are manifold. The electrical signal of the EEG is riddled with artifacts because of many ongoing processes – at the instrumentation level (currents induced in the EEG leads by gradient switching, etc.) as well as at the level of the human body (eye blink and BCG - ballistocardiogram - artifact) [3]. In addition, the MR image is adversely affected by the EEG electrodes and conductive leads.

1.3 Influence of EEG Electrode Cap on MR Images

Two types of noise and artifacts are generated in the MR images by the EEG electrodes, associated leads and the conductive material in the electrode chamber.

One type of artifact produced in MR images by electrodes and other EEG cap components arises from magnetic susceptibility mismatches, which in turn lead to

magnetic field inhomogeneities that cause focal signal losses due to spin dephasing and spatial intensity shifts in brain regions adjacent to the electrodes. These large, local magnetic field inhomogeneities interfere with proper image formation, since they dominate the desired linear gradient fields generated by the gradients. This artifact can be effectively reduced by careful selection of the materials used in the electrodes and leads to match the magnetic susceptibility of the head, by minimizing the size of components, and by increasing the distance between components made of materials of differing magnetic susceptibilities from the skull. But, as the EEG electrodes remain on the scalp and inside the field of view of the MR head coil, their impact on the MR images obtained should be understood well.

The second major source of noise and artifact in the MR image that is produced by EEG is RF noise injected by the EEG electrodes and leads acting as radiating radio frequency antennae. This can generate global reduction in the signal-to-noise ratio (SNR) of the image, as well as discrete noise patterns in the image. The global decrease in the SNR is depicted very aptly by Fig. 1.1, excerpted from a recent research paper [8]. However, there was no mention of the head coil that was used as a receiver.

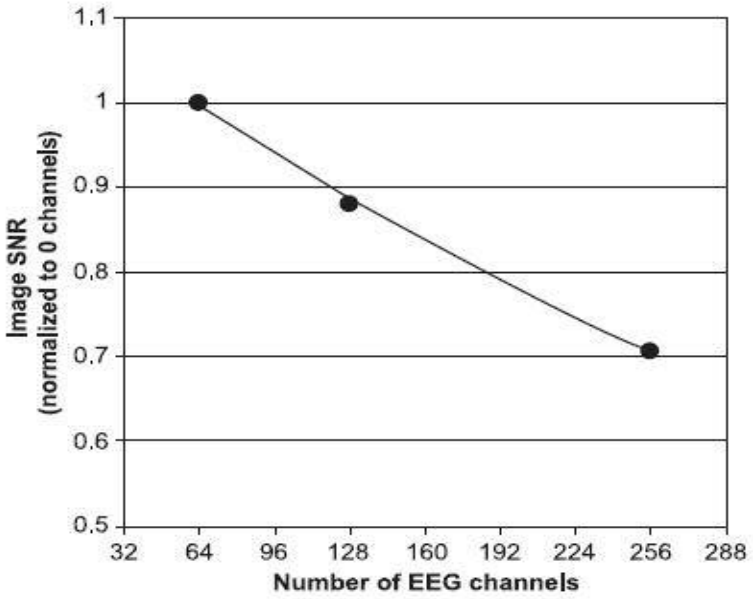

Figure 1.1 Drop in image SNR as a function of number of electrodes on EEG cap. Figure from reference [8*].

Other work that has been done till now to characterize the effects of EEG caps and electrodes on the MR images has been site specific, using EEG equipment that those research groups built in-house [5, 6, 7]. The widespread availability of commercially available MR-compatible EEG caps and systems from companies such as Compumedics-Neuroscan now makes it possible to systematically investigate the effect of EEG systems on a number of different MR head coils at different field strengths, and to more fully characterize and understand artifacts in MR images produced by EEG electrodes and leads. Although Neuroscan claims that, "Successful recordings and quality MR data have been obtained with MagLink systems containing from 37 to 128 electrodes" [10], there is only one study which has compared the effect of different

* Reproduced from Scarff et.al., Simultaneous 3-T fMRI and high-density recording of human auditory evoked potentials, Neuroimage, 23, 1129-1142, © 2004, with permission from Elsevier.

densities of EEG electrodes on the MR image SNR [8]. One site reports a similar study for a different vendor (SD-MRI, Micromed, Italy) [9]. The information pertaining to the EEG system and head coils used by various studies cited by this research project has been tabulated in Table 1.1 below.

Table 1.1 Studies that have explored the impact of EEG electrodes on MR images

Study	**MR system**	**EEG cap and System Vendor**	**Electrode array density**	**EEG cables**	**Type of head coil**
Krakow et al., 2000 (6)	1.5T Horizon, GE	In house	-	Copper	No Mention
Baumann et al., 2001 (5)	1.5T Signa, GE	Cap– Electrocap Intl.	64	Copper	No Mention
Bonmassar et al., 2001 (7)	3T GE	Cap – In house System – Neuroscan	64	-	EPI – Surface Anat. – Volume
Scarff et al., 2004 (8)	3T Signa, GE	Maglink, Neuroscan	64, 128, 256	Carbon - fibers	No Mention
Ianetti et al., 2005 (9)	3T Inova, Varian	SD – MRI, Micromed	32	-	Tx-Rx birdcage

None of the studies cited in Table 1.1 have discussed the impact that material from which the EEG cables are constructed might have on the MR images. Likewise, the interaction of the EEG electrode caps with different head coils has been ignored.

Our belief that some kind of analytical study of the equipment is necessary before embarking on full-fledged simultaneous EEG – fMRI experiments has led to this research project. The particular configurations of EEG cap, leads, and RF coil that we have in our lab have not been reported in the literature previously. In addition, no data

exist on the effect of different MR head coils on the degradation of SNR. This project was undertaken to fill in some of the blanks in the sparse and spotty literature that exists on this topic.

1.4 Aims and Hypotheses of This Research Project

The first aim is to test the effect of the electrode density, or number of electrodes, of the EEG electrode caps available to us on the MR image SNR, following the observations of Scarff et al. [8]. They found that the SNR of the images drops with increasing density of EEG electrodes (Fig 1). However, they used carbon - fiber cable leads, whereas we have copper - cables in addition to carbon - fiber cables. In addition, they tested 64, 128, and 256 electrodes, whereas we tested 32, 64, and 128 electrodes. The data point for a 256-electrode cap will be added when this electrode cap is available in our lab.

The second aim is to test the effect of two different EEG cables (carbon - fiber cable and copper - cable) on the MR image SNR.

The third aim is to test the effect of the two different head coils available in our laboratory: a 12 – channel receive coil (Siemens) and a transmit-receive quadrature or circularly polarized coil (USA Instruments).

The fourth aim is to better understand the impact of the EEG cap material and the conductive medium by testing the effect of the conductive saline medium used to lower the electrode impedance in the Neuroscan Quick Cells. This last question may not

be completely answerable, as the phantom is not conducting and there is no active electrical activity which could couple to the circuit and add noise as an additional rf antenna source.

It is hypothesized that:

1. The SNR will drop as a function of increasing number of EEG electrodes, for both the head coils.
2. The SNR will drop more when the carbon - fiber cables are used to connect the EEG cap to the head box (the amplifier) instead of copper - cable. This hypothesis is based on the fact that the copper - cable runs through a dedicated RF filter assembly connected to the penetration panel, whereas the carbon - fiber does not, but instead is passed through a waveguide in the penetration panel.
3. The SNR drop will be less for the 12-channel coil than for the quadrature transmit-receive coil because of the inherent electrical isolation of the array elements in the array coil.
4. The addition of saline solution to the Quick Cells in the EEG cap will add additional noise to the MR image.

The approach taken for performing the experiments and analyzing the data is described in the following Methods section. The results are presented and discussed in the section following that. The thesis ends with a Conclusion and a short section on future work suggested by this project.

CHAPTER 2

METHODS – HARDWARE

For simultaneous EEG – fMRI, both the EEG system and MR system are used in conjunction. The major components directly pertaining to the objective of this study are described later in this chapter.

2.1 The MR system

At the heart of the MR system is a superconducting magnet generating a strong static or DC magnetic field. The net magnetic moment (the magnetization) of the proton spins nutating at the Larmor radio frequency gets aligned with the main magnetic field. This arrangement of proton spins is perturbed by an external RF (radio frequency) source creating an oscillating magnetic field perpendicular to the magnetization vector and DC magnetic field. The spins gain energy and the magnetization vector gains components transverse to the DC field, which are detected by the RF receiver coils. The RF energy absorbed by the spins is eventually released to the surrounding environment or lattice via molecular interactions. For imaging the brain with an MRI scanner, the head coils are used as the RF receivers.

2.1.1. RF Head Coils

Different kinds of radio frequency head coils are used for different purposes and different head coils interact differently with the load (human head). Some head coils are

receivers only, in which case the transmitter is typically a separate, electrically decoupled body coil. Some coils serve as both transmitter and receiver. The size, design, and electric components of a head coil dictate its interaction with the head (and the EEG electrodes on the scalp) and the quality of the images so obtained.

There are two different head coils available in the lab – a 16-rung transmit-receive quadrature coil (Fig. 2.1(a)) manufactured by USA Instruments (Aurora, Ohio) and a 12-channel receive-only coil (Fig. 2.1(b)) manufactured by MRI Devices Corp. (Gainesville, FL), now InVivo (Latham, New York). For the latter, a body coil serves as transmitter, and the signals collected from each of the array elements are reconstructed and combined in data processing to form the image.

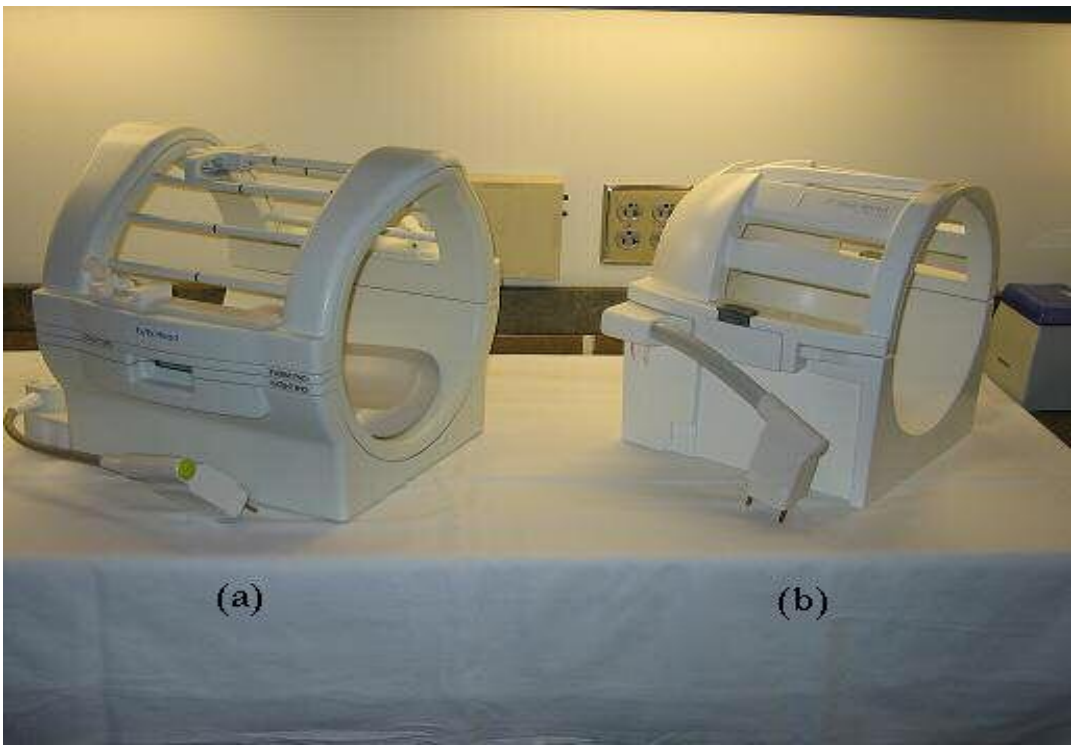

Figure 2.1 The two head coils used in this project: (a) a quadrature transmit-receive coil, (b) a 12-channel receive-only coil

2.1.2 Phantom

A phantom is used to load the head coil in the absence of an actual human subject. There are a variety of phantoms available for MR quality assurance (QA) tests. For this research project a plastic, 16-cm diameter spherical, silicone oil phantom was used for the experiments. This phantom actually belonged to a GE scanner in the imaging facility. A silicone oil phantom was chosen because:

a. It offers better RF uniformity due to its low dielectric constant than an aqueous phantom doped with $NiSO_4$, with high dielectric constant that produces non- uniform signal intensity due to dielectric resonances [11].

b. As oil is denser than water, the liquid inside the phantom takes less time to stabilize (to settle down after turbulence because of movement).

The phantom was wrapped in a flimsy sandwich wrapping plastic sheet (*Saran Wrap*) to avoid spoiling the phantom with saline solution[*]. As the wrap was very thin, it stuck to the phantom nicely. The loose ends were taped with a medical tape. Use of medical tape was kept to bare minimum.

As shown in Fig. 2.2, the phantom had two labels from the manufacturer which were left untouched for the experiments. These labels also served the purpose of major positioning indicators while land-marking the phantom before each scan. The red arrow in Fig. 2.2 points to the *snout* (severed cap) of the phantom. This end of the phantom was always towards the foot of the patient table.

[*] This phantom is also used for routine quality assurance at the Meadows MRI facility.

Figure 2.2 Silicone oil phantom used in this thesis project

2.2 The EEG system

Traditionally, EEG systems have comprised of a set of electrodes that go on a subject's head (scalp), an amplifier which is fed the electrical signals coming from all electrodes through conductors in a cable, and a data acquisition system which records the EEG signal waveforms (Fig. 2.3). The electrodes are placed on the scalp of the subject and an electrolytic gel is introduced into the electrode cavity (or, in the case of the Neuroscan Quick Cells, the sponge in the electrode cavity is soaked with saline solution) to create a conductive column from scalp to electrode [5]. The setup and major components have remained essentially the same even for the MR-compatible EEG systems.

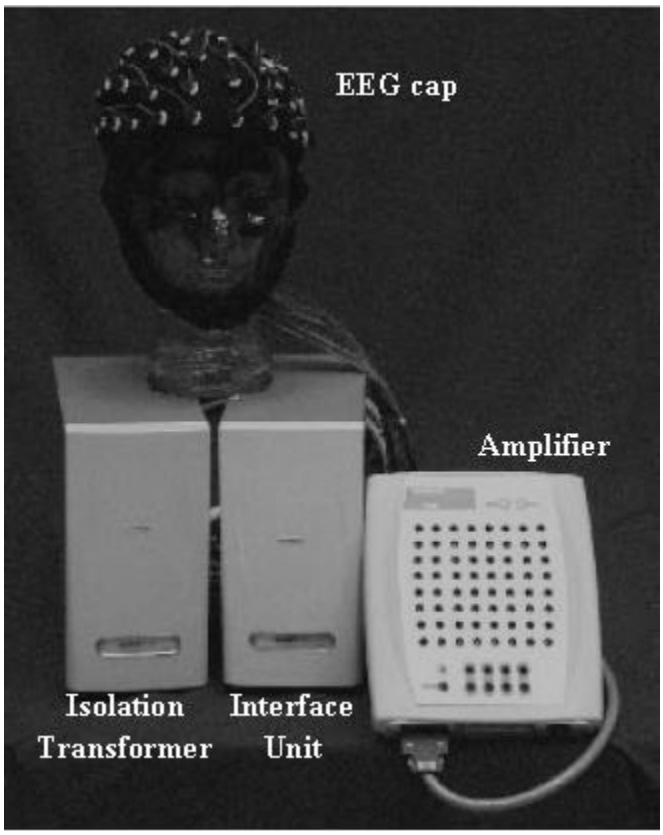

*Figure 2.3 Major components of an EEG system minus the data acquisition computer.

The only part of the system that is inside the MRI magnet room is the EEG electrode cap and the associated conductor cables. Almost all the electrically active components (amplifier, interface unit, isolation transformer, and data acquisition system) of the EEG system usually are not in the magnet room, but are rather in the MRI scanner control room, as is shown in Fig. 2.4.

* Figure adapted from Neuroscan Product Notes – manual 7228C

Figure 2.4 Components of the EEG system that are in the control room
(a) data acquisition system (b) isolation transformer (c) interface unit
(d) amplifier (e) RF filter assembly

2.2.1. EEG Electrode Caps

The electrode cap (Fig. 2.5) for the Maglink RT system is made of highly elastic fabric. This cap is fitted with sintered silver-silver chloride electrodes according to the advanced 10-20 system. There is a small cavity in each electrode holder which holds the cellulose sponges (quick cells) in place. This cavity is connected to the back of the electrode holder via a hole in the holder. It is this hole through which the conducting

medium (saline) is introduced into the quick cell in the cavity. On salination, the quick cells expand within the cavity and form a continuous conductive column from scalp to the electrode.

Figure 2.5 Maglink RT EEG electrode cap with connectors

The EEG electrodes, the electrolytic gel or saline-soaked sponges, and (part of) the conducting wires from the EEG electrodes to the amplifiers are inside the RF coil that is placed in the magnet to receive MR signals from the brain during MR imaging. It is the interplay of these EEG hardware components with the main magnetic field, gradient fields, and RF head coil which causes the degradation of the brain images obtained from the MRI scanner in a simultaneous EEG-fMRI experiment.

In an actual experiment, the amount of saline that goes in each quick cell varies according to the behavior of the impedances of each electrode site. But, for this study, 100 μl of saline was introduced into each quick cell using a programmable electronic

pipette. This was done to ensure that no saline spills out on the phantom and no bridges are formed between two adjacent electrodes.

The red wires (in Fig. 2.5) are the leads which run from every electrode to the circular multi-pin connectors leading to the cables. All the leads are non-ferrous and carbon - fiber based. Right near the electrode, there is a 6.8 k-Ohm resistor in series with the lead. This resistor helps to ensure patient safety in case any current loops form in the leads inside the scanner magnetic field. As a precaution, these leads have been twisted around each other to help prevent induced current loops from forming.

There are three pairs of electrodes which are not physically on the EEG cap body, but hang loose – two mastoid electrodes, a bipolar electrode pair for recording eye movements (the EOG – electro-oculogram), and a bipolar electrode pair for recording electrocardiogram (EKG). On the wrapped phantom, these electrodes were attached sufficiently apart from each other and such that the general placement of these electrodes is maintained similar to what would be used in a human experiment. Thus the two EOG electrodes went on the anterior face of the phantom, the two mastoid electrodes went in the ear region of the phantom, and the two EKG electrodes went in the neck area - all as demarcated by the EEG cap chin straps.

Three sizes of EEG electrode caps were available at the lab – small, medium and large. A small sized cap was used for all the experiments in this project as it hugged the phantom best.

2.2.2. EEG Cables

Our lab has two sets of conductor cables which run from the EEG electrode cap inside the scanner room to the amplifier setup (head box) outside the scanner room – the Maglink RT cable (Fig. 2.6(a)), which is a copper - cable, and a carbon - fiber cable (Fig. 2.6(b)).

The Maglink RT cable is a flexible cable made of copper alloy. One end of this cable is connected to the passive adapter (red arrow in Fig. 2.6), which in turn is connected to the connector of the EEG electrode cap. The other end of the cable is connected to the RF enclosure assembly as described in section 2.3.2.

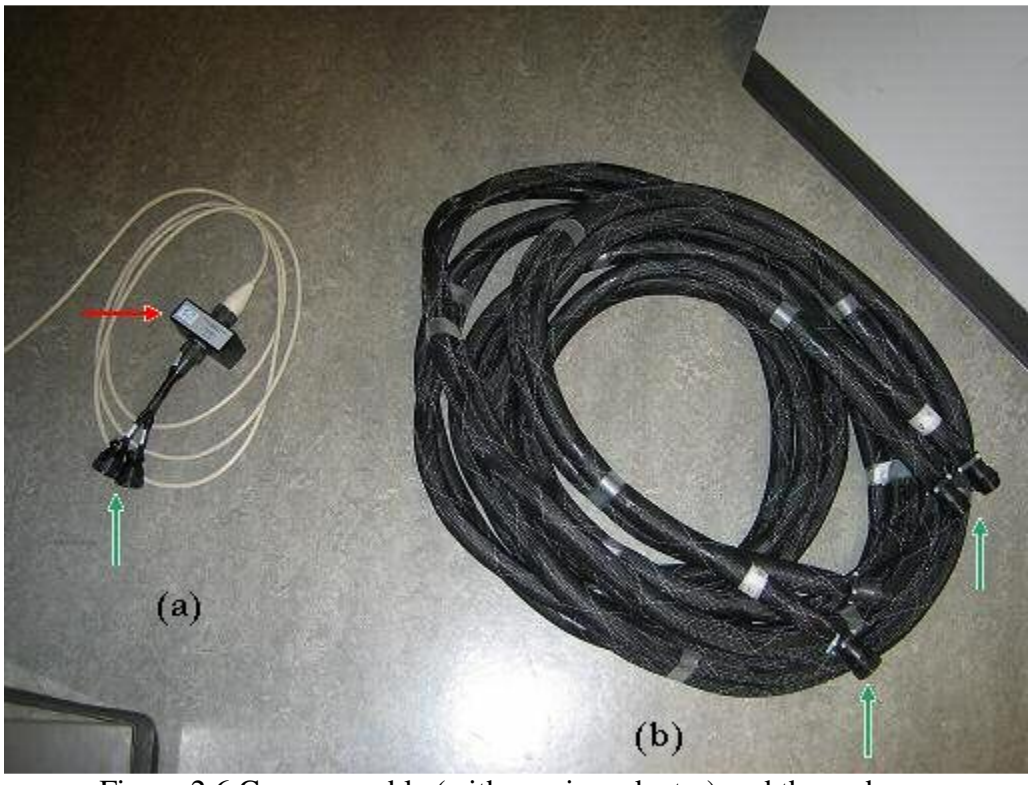

Figure 2.6 Copper - cable (with passive adapter) and the carbon – fiber based cable.

The carbon - fiber cable is a bulky set of two cables (snake cables). It is connected to the EEG electrode cap circular multi-pin connectors on one end and to a adaptor at the other end, inside the scanner room. The adaptor helps convert the cable from circular multi-pin connectors to a rectangular multi-pin connector system. The rectangular pin connector is hooked up to the penetration panel through an RF filter.

The connectors of both the cables that connect to the EEG cap are the same kind (green arrows in Fig. 2.6). In both cases, the cables coming from the 64-channel cap are composed of two groups of 32 leads, each group with a 32-pin connector of its own. The braided bunch of leads coming out from the EEG cap is all carbon - fiber. The cables shown in Fig.2.6 are the ones that connect to the 64-channel EEG cap. These cables were also used to connect the 32-channel as well as 128-channel EEG caps to the amplifiers. For the 32-channel EEG cap, only one of the two 32-channel cables and its 32-pin connectors were required, as there were half the number of electrodes on the EEG cap. The *spare* connector on the second cable was left unconnected. For the 128-channel EEG cap (which has four 32-pin connectors) only two of the connectors coming out from the EEG cap were used. Care was taken in ensuring that half of the electrodes on each hemisphere of the EEG cap were connected for every scan session where the EEG cap was on the phantom.

2.3 Simultaneous EEG – fMRI System

The high magnetic fields of MRI scanners make it imperative to have equipment for simultaneously recording EEG that is compatible with the MR magnet and

environment. A number of research groups across the globe have tried to develop such systems in-house. As the number of research facilities using EEG in conjunction with fMRI has increased, MRI - compatible EEG systems have become available commercially. The MR-compatible EEG system that was used for this research is from Neuroscan (a division of Compumedics), El Paso, Texas. The interfacing of the separate modalities needed for a system to simultaneously record EEG signals and MR images – an EEG system and an MRI system - is depicted in the schematic shown in Fig. 2.7.

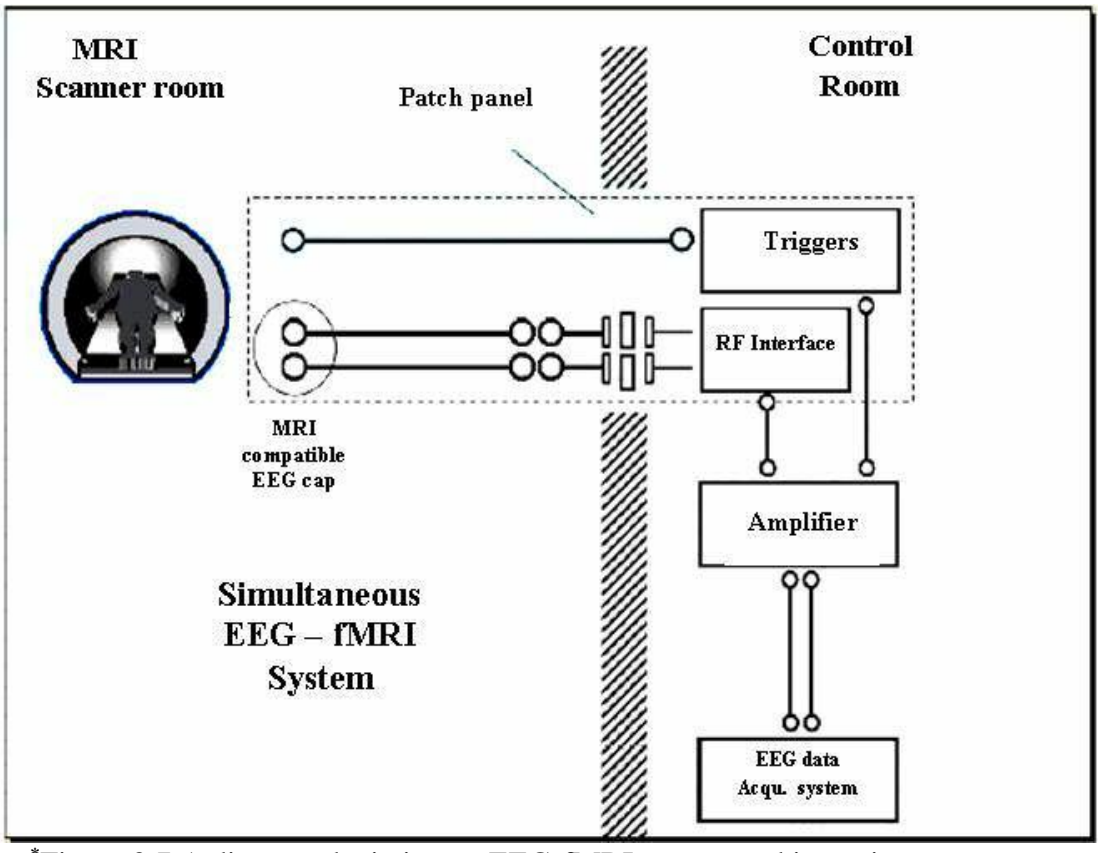

*Figure 2.7 A diagram depicting an EEG-fMRI system and its major components

* Figure adapted from Neuroscan Product Notes – manual 7228C

2.3.1. The Penetration Panel

The penetration panel (or patch panel) is the only mode of electrical communication between the scanner room and the control room during an MRI scan. It is a thick brass sheet which houses a number of filtered electrical connectors to facilitate connections of the secondary equipment inside the scanner room to respective control systems in the control room (e.g., response pads, audio - visual communication systems, physiological monitoring systems, EEG data acquisition system, etc.) without RF interference.

The cables running through the penetration panel could provide a pathway for the unwanted RF signal from outside the magnet room. To reduce this possibility, RF filters are used in the panel for various connectors. RF filters for many different types of connectors (serial, parallel, BNC, VGA, DB-9, DB-25, DB-37 etc.) are pre-mounted on the penetration panel as depicted in Fig. 9(a).

The EEG cable runs through the penetration panel into the long black waveguide which connects to the RF enclosure assembly as can be seen in Fig. 2.8(b).

Our lab has two sets of conductor cables which run from the EEG electrode cap inside the scanner room to the amplifier setup (head box) outside the scanner room – the Maglink RT cable (Fig. 2.6(a)), which is a copper - cable, and a carbon - fiber cable (Fig. 2.6(b)).

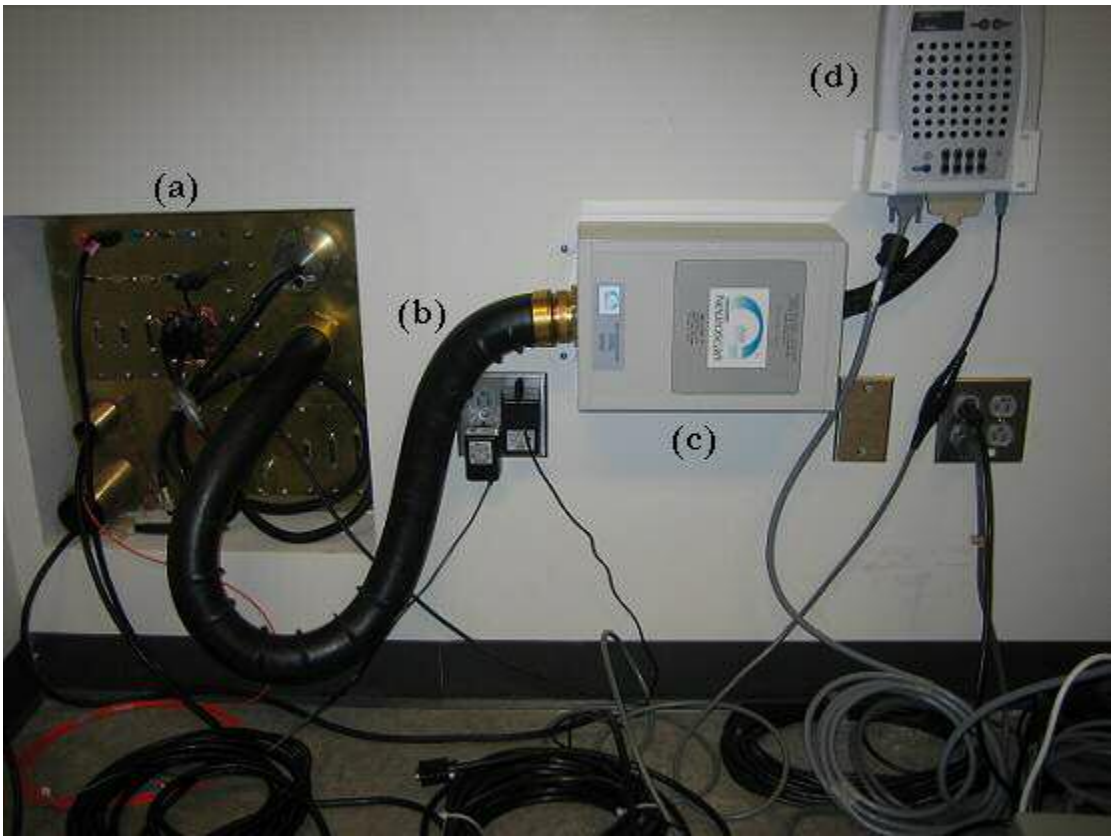

Figure 2.8 Parts of the EEG equipment in the scanner control room
(a) RF penetration panel (b) waveguide (c) RF enclosure (d) head box
(b) (EEG amplifier)

2.3.2. The RF Enclosure Assembly

The RF enclosure (Fig. 2.8(c)) is a metal box mounted on the wall near the RF penetration panel in the control room. It is part of the Maglink RT EEG system. It serves the purpose of keeping any stray RF generated by the EEG equipment in the control room from riding the EEG cables and into the scanner environment. A special waveguide (Fig. 2.8(b)) connects the penetration panel waveguide to this enclosure. The purpose of this waveguide is to prevent any kind of electrical coupling between the scanner room and the control room. The RF enclosure has copper wire meshes inside it connected at the input and the output ends. The output end of the RF enclosure connects

to the cable from the head box (Fig. 2.8(d)). This cable is also covered end to end with a braided fine wire sheath for keeping out the RF.

CHAPTER 3

METHODS - EXPERIMENTS

The basic experiment consisted of three different conditions:

(a) MRI image acquisition without an EEG cap.

(b) MRI image acquisition with EEG cap but without any kind of conductive medium (saline) inside the electrode cavity.

(c) MRI image acquisition with EEG cap and with a conductive medium inside the electrode cavity.

Three different densities of EEG electrodes (32, 64 and 128 electrodes), two different head coils (12-channel receive coil and 16-rung transmit-receive quadrature coil) and two different sets of cables (copper - cable and carbon - fiber cable) for the EEG system were used for the three separate conditions (phantom alone, phantom with EEG cap, and phantom with EEG cap with saline). The total number of image acquisition scans was 36 (3 electrode caps x 2 RF coils x 2 cable types x 3 conditions). All the scans for one electrode density EEG cap were completed in the same scanning session.

Only one measurement (N = 1) was performed for each condition i.e. the measurements for different conditions were not repeated. Every time the phantom was removed from the head coil, 3 – 5 minutes were allowed for the liquid (silicone oil) inside the phantom to stabilize before performing the next scan.

As the reproducibility of placement of the electrode cap on the phantom was deemed important, conditions 2 and 3 described above were performed for both head coils one after the other. Then the cables for the EEG system were switched and all the image acquisitions were performed again. A simple chronological flow-chart (Fig. 3.1) describes the order of all the scans for one scanning session.

To minimize the possibility of systematic errors over the experimental sessions, the following precautions were taken:

(a) The order in which the head coils were switched within each of the three sections labeled as A, B and C in the flowchart was varied.

(b) Over three days (for three different electrode density caps), the section A of the experiment was performed either in the beginning of the session or at the very end of the session (after stripping the electrode cap and plastic wrap off of the phantom).

(c) Over three days (for three different electrode density caps), the order of performing sections B and C was varied as well.

(d) The two sets of cables were used first in the scanning sessions alternatively.

The image acquisitions without the EEG cap were performed either at the beginning of a session or at the very end of a session. This was done so that the positioning of the EEG electrode cap could be reproduced while using different head coils.

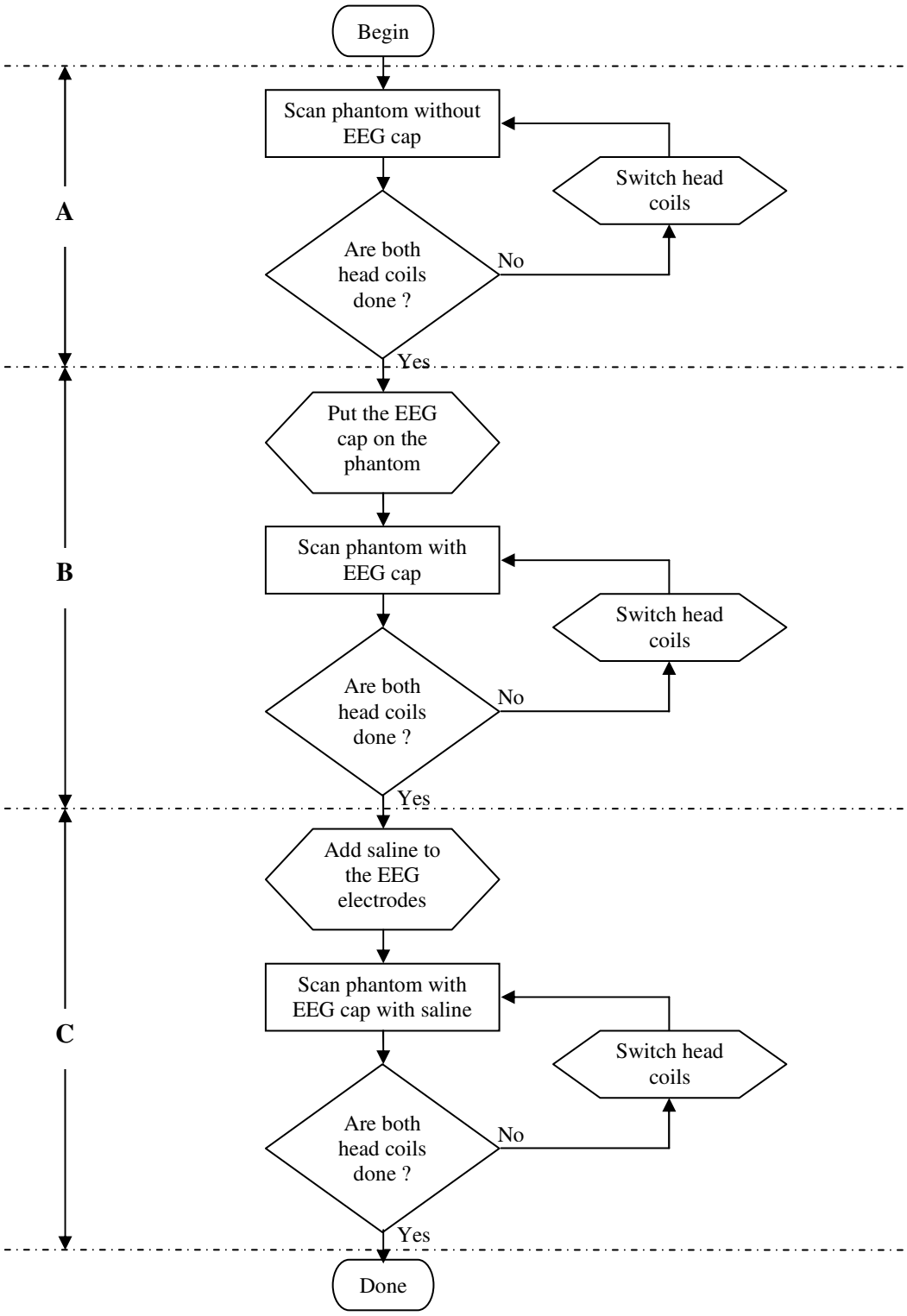

Figure 3.1 Flow chart depicting scans undertaken for single electrode density cap.

3.1 The Experimental Setup

For the image acquisition without EEG cap, the phantom was placed in the head coils. Foam pads from the scanner room were used to center and stabilize the phantom in the head coil.

Three different sizes of EEG caps were available with the Neuroscan EEG system – small, medium and large. The small electrode cap was put on the plastic-wrapped phantom, as it fit the phantom best. Once the cap was on, the chin straps were tightened according to the pre-marked landmarks on the plastic sheet that was wrapped around the phantom. The phantom with cap was placed in the head coil. Position of the phantom was centered using the padding available in the scanner room. The method of padding was noted down diligently the first time and it was followed as closely as possible for all subsequent sessions with same head coil for all three conditions (without EEG cap, with EEG cap but without saline, with EEG cap and saline).

For the scanning sessions with the EEG cap, quick cells (cellulose sponges) were introduced into slots in the electrodes manually before each session. After scans with EEG cap on the phantom were finished, the setup was taken out of the head coil and saline was pipetted into all the quick cells as has already been mentioned in Section 2.2.1 namely EEG electrode caps.

Once inside the head coil, the phantom was land-marked with the scanner's laser – beam cross hair and the patient table was sent inside the bore of the magnet. For a given head coil, as far as was possible, the land-marking was done in the same

position on the phantom for each scan session (using the two labels described earlier as indicators).

3.2 Image Acquisition

The phantom (with and without EEG cap) was scanned in three different slice orientations – axial, sagittal and coronal. fMRI experiments acquire brain images in different orientations depending factors such as the brain region of interest and the brain coverage required. As the EEG electrode cap only partially covers the phantom (and human head), it was thought that images in different orientations would be affected differently. Three-slices were acquired for each orientation, with the middle slice centered at the central axes intercept of the phantom. For all the scan sessions, a GRE (gradient echo) 2-D FLASH (Fast Low Angle Shot) sequence with active RF spoiling was used. The detailed parameters of the scan protocol are as follows:

TR	=	1500 ms
TE	=	4.5 ms
Flip Angle	=	90 [deg]
Slices	=	3
FoV Read	=	256
FoV Phase	=	100.0% (256)
Base Resolution	=	128
Phase resolution	=	100.0% (128)
Slice Thickness	=	5 mm
Dist. Factor	=	400% (20 mm)

Band Width	=	200 [Hz/Px]
Averages	=	1
Concatenations	=	1
Slice Orientation	=	Axial, Coronal, Sagittal

3.3 SNR Measurements

After image acquisition was complete, the signal and background noise measurements were made. Signal was measured from a centrally placed circular ROI (region of interest) and four other peripheral ROIs at the top, bottom, right, and left of the image, as shown in Fig. 3.2. Care was taken in placing these four ROIs in the phantom field such that each ROI was spaced equally from the centrally placed ROI as well as from the wall of the phantom. Each of the four peripheral ROIs was about 5 – 7 mm away from the phantom wall. The position of the five signal ROIs ('S1' thru 'S5' marked in green in Fig. 3.2) remained the same for same orientation scans for different experimental conditions on the same day. The ROIs for background noise measurement (the ROIs marked with letter 'N' in red in Fig. 3.2) were placed in corners of the FOV (field of view). All the ROIs were placed at the same position for all three-slices of one scan. The viewer on the scanner console annotates mean and standard deviation values from the ROIs. The mean value and standard deviation of the signal ROIs as well as background noise (standard deviation of noise ROI) were noted down in a data acquisition/measurement sheet.

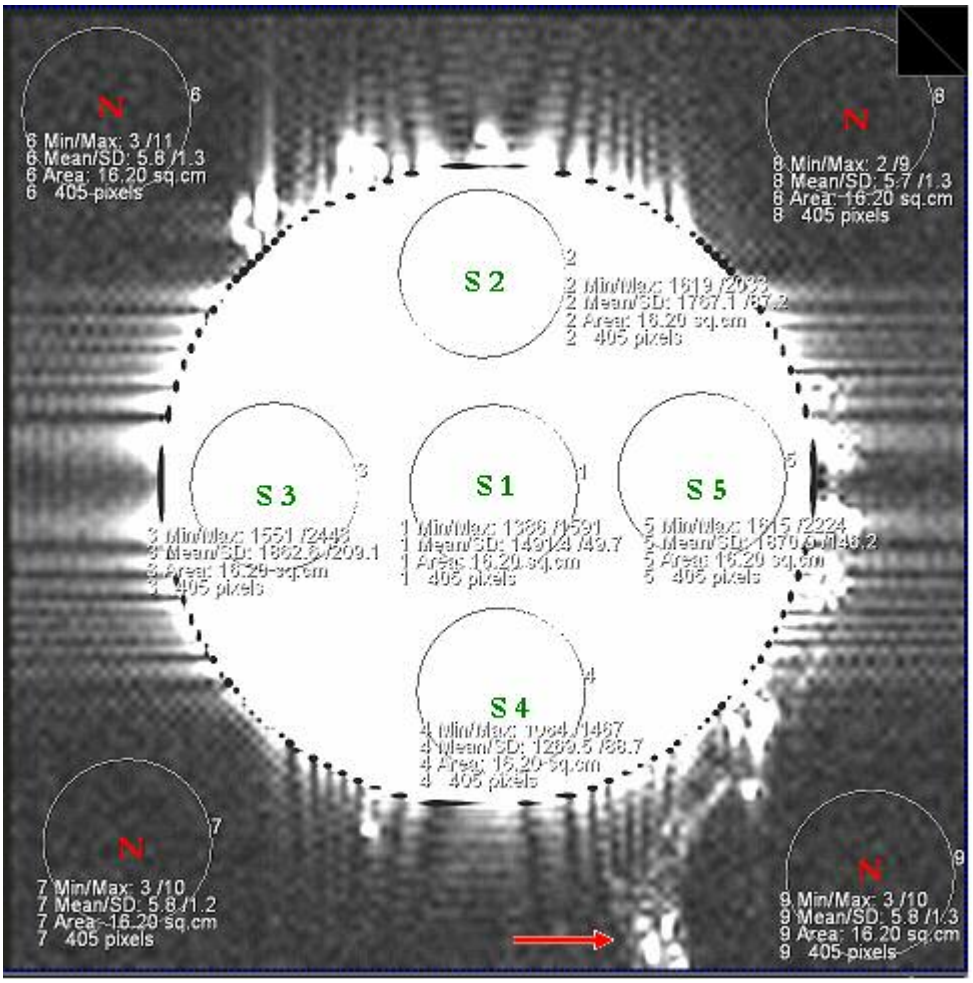

Figure 3.2 Placement of multiple noise ROIs (N) and five signal ROIs (S1 thru S5) in the FOV.

As other artifacts such as ghosts (in phase encode direction) invariably show up in the MR images, it is important to avoid those artifacts while making the background noise measurements. The ROIs for background noise measurement were always placed in a corner of the FOV (Fig. 3.2). At times, the choice of corner for background noise measurement was limited because the electrode leads bundle ran from one of the corners of the FOV in coronal and sagittal slice orientation (as pointed to by the red

arrow in Fig. 3.2). Note that saline in the Quick Cells is also visible around the periphery of the phantom in the cap.

The size of the ROIs for background noise measurement as well as signal measurement was kept the same as much as was possible. Size of the ROIs was always between 436 – 475 pixels - about 10% of the size of the phantom image through its biggest diameter.

The SNR was calculated according to the following relation:

$$SNR = \frac{S-N}{\sigma}$$

Where, SNR is signal-to-noise ratio, S is mean signal measured from the signal ROI, N is mean noise intensity in the magnitude image, measured from background ROIs, and σ is the standard deviation of the noise.

CHAPTER 4

RESULTS AND DISCUSSION

There were four primary goals of this thesis project:

1. To see the effect of increased density of EEG electrodes on the MR image SNR.
2. To study the effect of two different EEG cables on the MR image SNR.
3. To study the effect of EEG electrode cap on MR image SNR in two different head coils available in the lab.
4. To study the effect of saline-laden quick cells in the EEG electrodes on the SNR of the MR images of the brain.

All the numbers that have been plotted are from only one measurement for all the different experimental conditions (N = 1).

The results are presented and discussed further in this section in the same order. To reduce clutter in the figure, only positive standard deviation bars are shown. The positive standard deviation bars in all the plots in this chapter depict the deviation obtained during averaging SNR values measured for an ROI across 3 slices for a scan unless otherwise mentioned. Pair-wise T-tests with an alpha of 0.05 were performed for the comparisons between different conditions. But, as there were three different orientations of scans, three slices for each scan and five ROIs for signal measurement, it

was thought that there could be some over estimation of the significance from the p – values so obtained from the pair – wise t – tests performed for fifteen ROIs per scan over different conditions. Thus, the Bonferroni Correction for the alpha was done to obtain the corrected alpha (0.05 / 15 = 0.0033). This alpha has been used to test for significance in the following sections of this chapter, unless otherwise mentioned.

In the first section of this chapter (4.1), the absolute average SNR obtained for all ROIs across three slices with the associated standard deviation as well as the normalized SNR has been depicted in the plots. In sections 4.2 – 4.4, only the absolute SNR has been plotted. In the last section (4.5) of this chapter, for sake of convenience of understanding, only normalized SNR has been plotted.

For quality control purposes, for each scanning session, the phantom was scanned alone and the SNR for three sessions was compared. Fig. 4.1 below is a plot for SNR of all five ROIs (as described in section 3.3 earlier) from scans from all three orientations – axial, coronal and sagittal for the 12-channel coil.

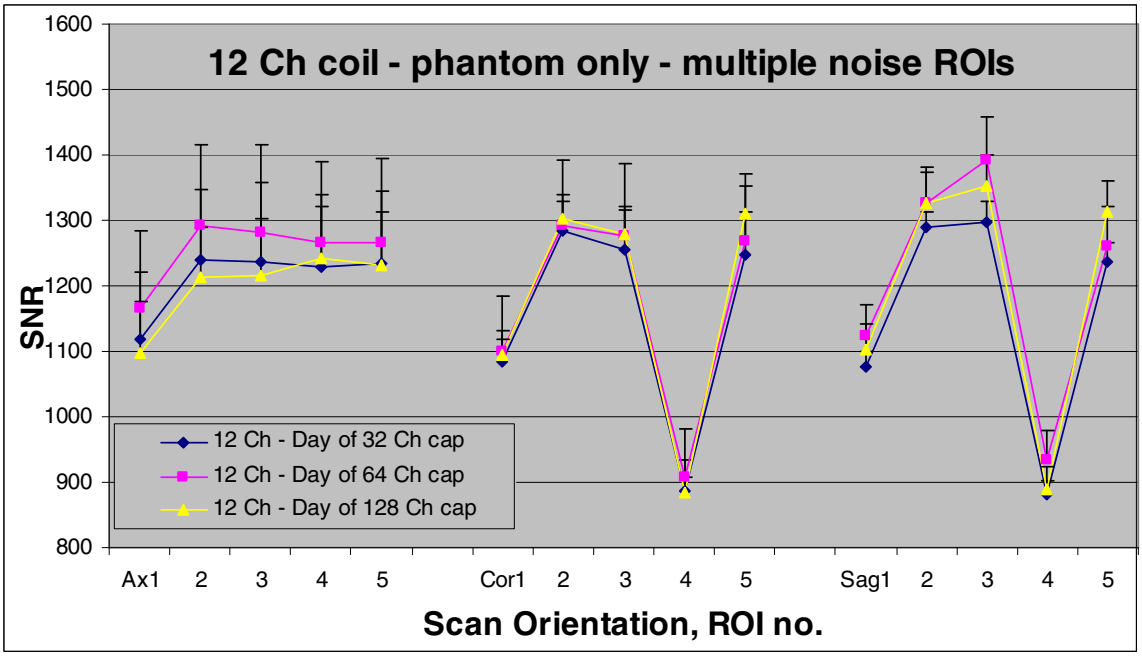

Figure 4.1 Plot of SNR for phantom only condition for all three scan sessions with 12–channel receive-only coil.

Although it appears from Fig. 4.1 that the system behaved the same way on all three days but, from the results of pair – wise t – tests (Table 4.1) conducted among the SNR values for scans done on three different days using the 12-channel rx-only coil for ROIs in all three scan orientations reveals that there was significant variation only between the phantom scans for $\mathbf{P_{Day\ 32}}$ (the day 32 – channel EEG cap was used) and $\mathbf{P_{Day\ 64}}$ (the day 64 – channel EEG cap was used) but not between $\mathbf{P_{Day\ 64}}$ and $\mathbf{P_{Day\ 128}}$ (the day when 128 – channel EEG cap was used) or between $\mathbf{P_{Day\ 32\ and}}$ $\mathbf{P_{Day\ 128}}$ So, the variation in the data discussed later in this chapter because of scanner instability cannot be entirely ruled out.

Table 4.1 Results of pair-wise t-test amongst SNRs of phantom-only condition, on three different days of scanning, for 12-channel receive - only coil.

	$P_{Day\ 32}$ vs. $P_{Day\ 64}$	$P_{Day\ 64}$ vs. $P_{Day\ 128}$	$P_{Day\ 32}$ vs. $P_{Day\ 128}$
p – value (one tail)	3.65E-06	0.03	0.02

For all three scan orientations, reduced SNR (lower by about 15%) was consistently noted for the central ROI (no. 1) as compared to other peripheral ROIs (nos. 2, 3 and 4). This could be due to the smaller effective penetration depth of the smaller sized array coil elements, compared to the larger transmit-receive coil. The smaller B1 in the center of the phantom for the 12-channel array coil compared to the periphery would produce less SNR in the center compared to the periphery. In contrast, the B1 of the larger transmit-receive coil is more spatially uniform from periphery to center. In addition, for coronal and sagittal orientation scans, for the ROI no. 4, there is a marked (about 30%) decrease in the SNR on all three days. Although care was taken to center the phantom in the coil, perhaps it was lower than centered. Another possibility is that the bottom coil element(s) is (are) different from the rest in terms of circuit properties.

Fig. 4.2 below shows the plot of SNR of the phantom-only condition for scans in all three scanning orientations for all three days that the scanning was done with the transmit-receive coil.

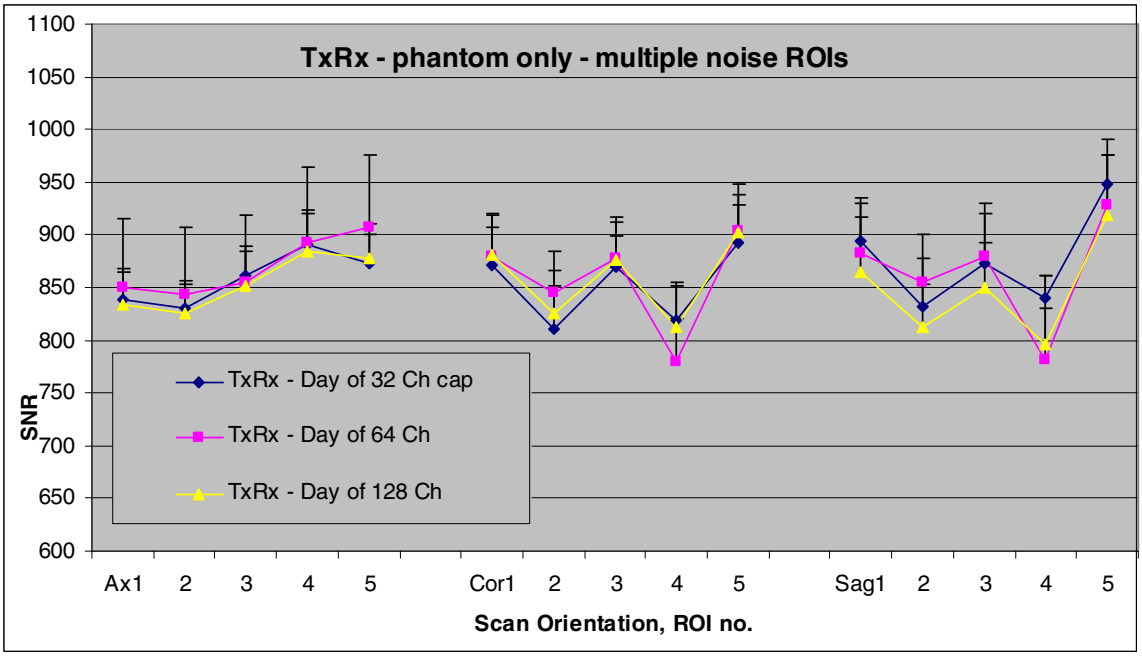

Figure 4.2 SNR for phantom only scans on all three days with transmit-receive coil.

From table 4.2 it is apparent that the difference between SNR for the scans of the phantom done using tranmsit – receive coil were not significant at all.

Table 4.2 Results of pair-wise t-test amongst SNRs of phantom only condition on three different days of scanning, for transmit - recieve coil.

	$P_{Day\ 32}$ vs. $P_{Day\ 64}$	$P_{Day\ 64}$ vs. $P_{Day\ 128}$	$P_{Day\ 32}$ vs. $P_{Day\ 128}$
p – value (one tail)	0.43	0.03	0.03

As shown in Fig. 4.2 as well as in Table 4.2, for the transmit-receive coil, the SNR follows the same pattern across all three scan sessions and the differences between the phantom-only SNR for $P_{Day\ 32}$ vs. $P_{Day\ 64}$, $P_{Day\ 64}$ vs. $P_{Day\ 128}$, and $P_{Day\ 32}$ vs. $P_{Day\ 128}$ were not significant.

Two interesting things were observed about the SNR values for the 12-channel receive-only coil. First, the central ROI consistently shows a smaller SNR value than

the peripheral ROIs. Second, the SNR for ROI no. 4 is significantly less than for the other three peripheral ROIs for the coronal and sagittal slice orientations. In coronal orientation scans, ROI no. 4 was inferior in position to the centrally placed ROI and for the sagittal orientation scans, ROI no. 4 was posterior to the centrally placed ROI. This behavior was not noted for the transmit-receive coil, for which the SNR was more consistent across ROIs and slice orientations.

A point to be noted while looking at the plots which compare the SNR for three different density EEG arrays is that the cables used to connect the EEG caps to amplifiers were meant to be used with a 64-channel EEG array system only. When the 32-channel EEG array was used, one of the connectors on either end of the copper - cable (or the carbon-fiber cable) was loose (not-connected). And when the 128-channel EEG array was used, two connectors on the EEG cap were loose (not-connected).

4.1 Effect of Increased Density of EEG Electrodes on MR Image SNR

The results for the effect of increased density of EEG electrode array on the MR image SNR are discussed in this section.

4.1.1 12-Channel Receive-Only Coil

The plots in Figures 4.3 and 4.4 depict the absolute and normalized SNR (SNR with electrode cap divided by SNR without electrode cap) respectively, for the 12-

channel receive-only head coil when the EEG cap is on the phantom and the copper - cable was used.

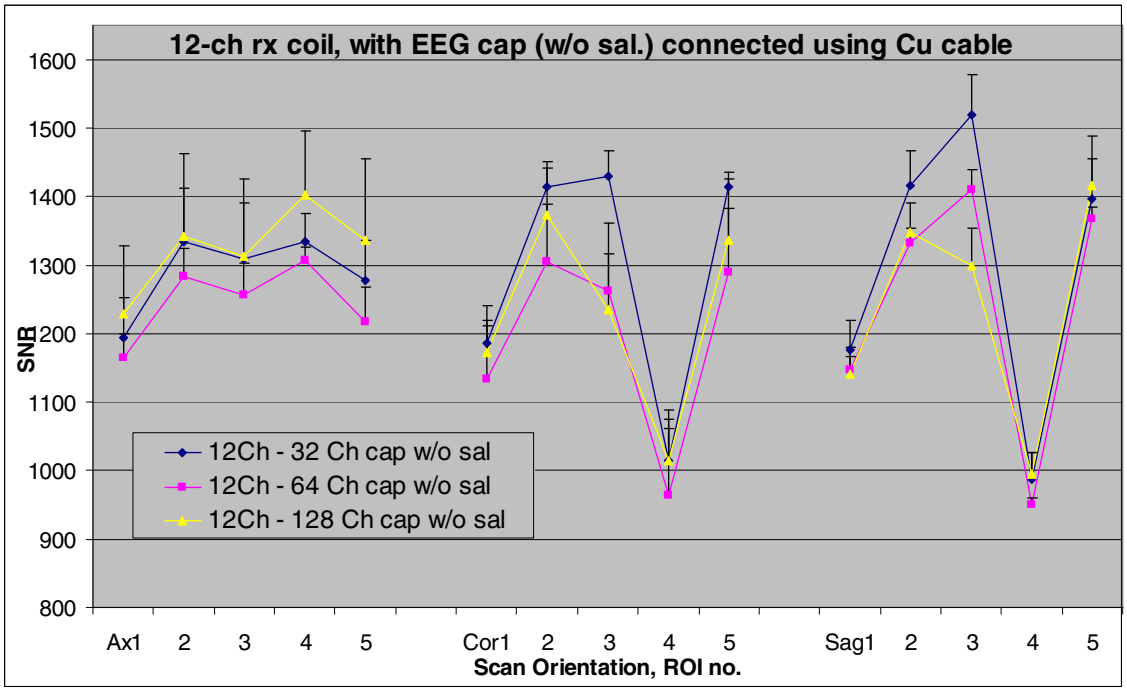

Figure 4.3 Comparison of absolute SNR for all 3 EEG electrode density caps for the 12-channel rx-only head coil, when copper - cable was used.

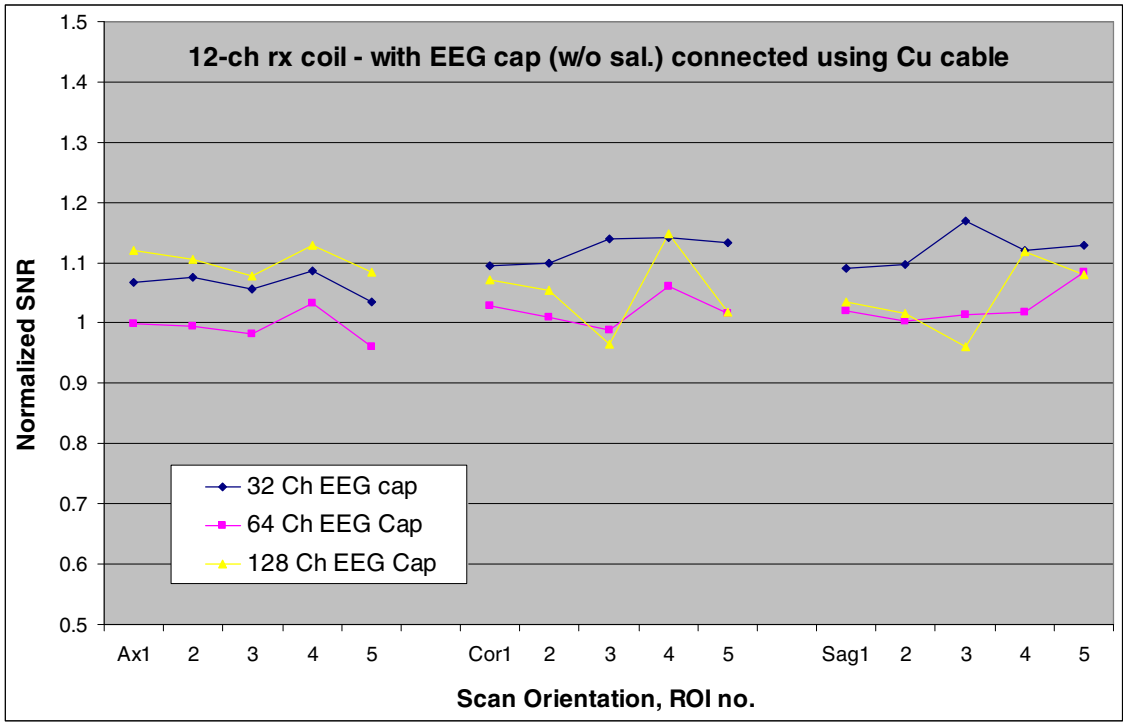

Figure 4.4 Comparison of normalized SNR for all 3 EEG electrode density caps for the 12-channel rx-only head coil, when copper - cable was used.

The plots in Figures 4.5 and 4.6 depict the absolute and normalized SNR (SNR with electrode cap divided by SNR without electrode cap) respectively, for the 12-channel receive-only head coil when the EEG cap is on the phantom and the carbon - fiber cable was used to connect the caps to the head-box (amplifier).

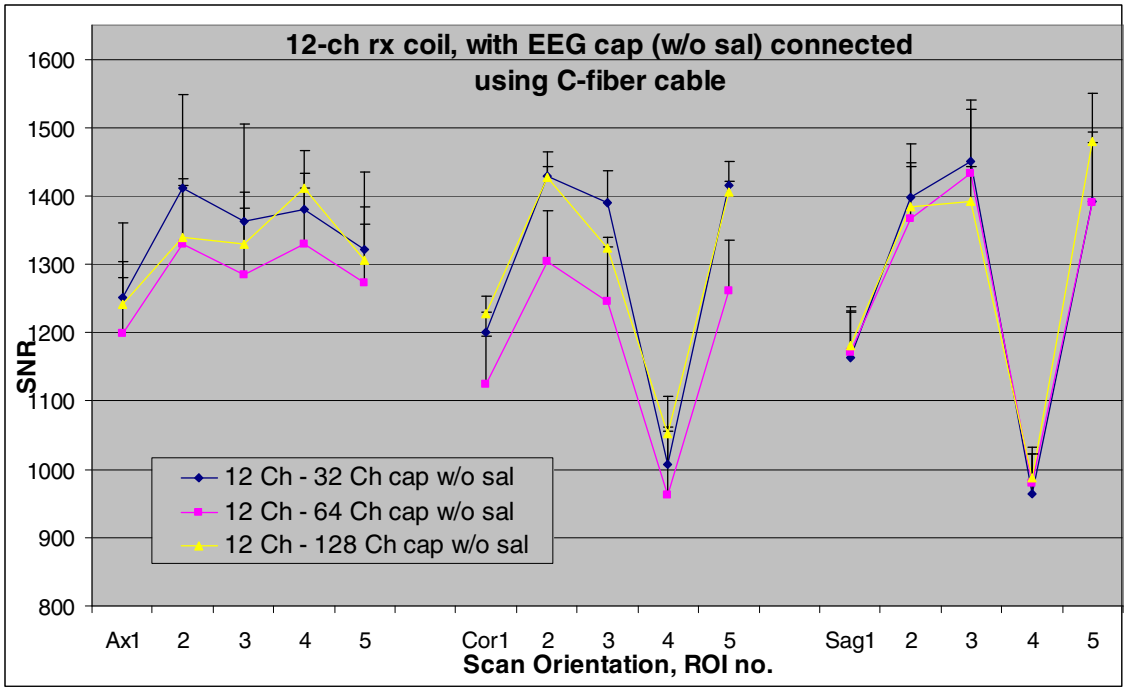

Figure 4.5 Comparison of absolute SNR for all 3 EEG electrode density caps for the 12-channel rx-only head coil, when carbon - fiber cable was used.

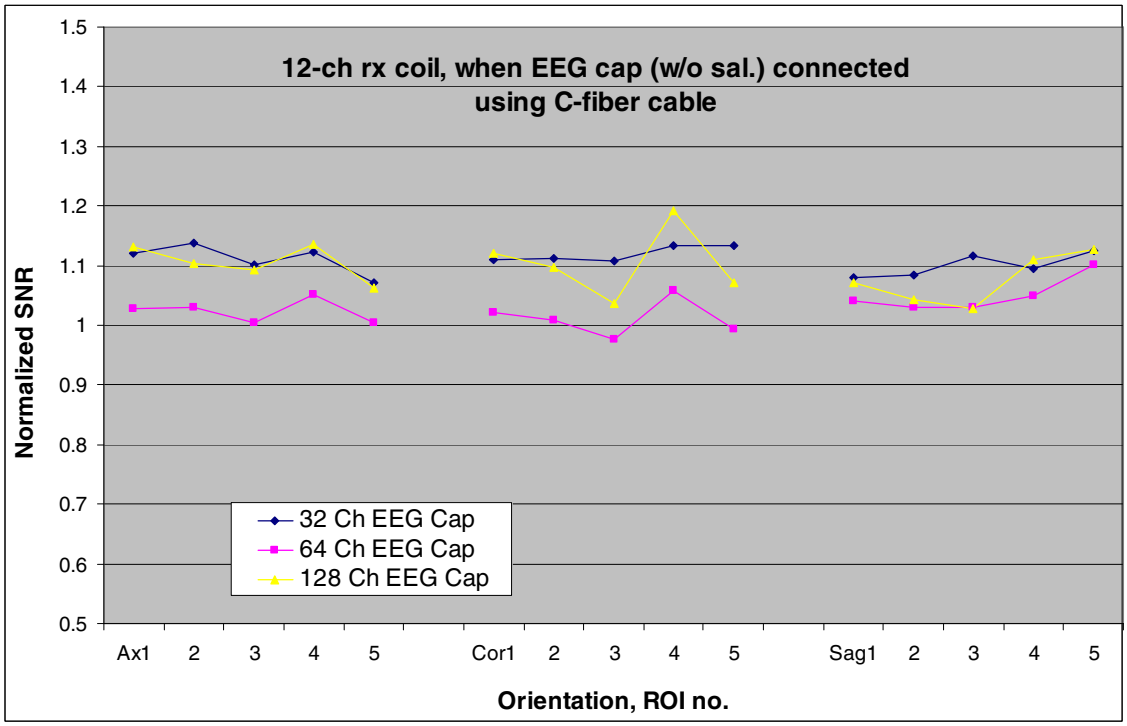

Figure 4.6 Comparison of normalized SNR for all 3 EEG electrode density caps for the 12-channel rx-only head coil, when carbon - fiber cable was used.

When the pair-wise t-tests were conducted on the phantom-only condition to the phantom with EEG cap condition while the 12-channel rx-only coil was being used, it was found that the SNR is often about 10% higher with EEG electrodes than without, except for the 64-channel EEG cap, for which SNR is little changed..

Table 4.3 shows p-values for 12-channel receive-only coil SNR data for the comparison of SNR with EEG cap to without EEG cap, for the three EEG caps and two types of cables. The increased SNR for the phantom with EEG cap compared to the phantom alone is significant in the order 32 > 128 > 64 electrodes for both cables, with the significance greater for the copper - cable than the carbon - fiber cable. For the 64-channel EEG cap with carbon - fiber cable, the change in SNR did not attain significance. But, in every EEG cap's case the normalized SNR for the phantom with EEG cap condition was not less than the phantom alone condition for the 12 – channel receive – only coil as the data points for the plots in Figures 4.4 and 4.6 show.

Table 4.3 Results of pair-wise t-test between SNR of phantom (P) and SNR of phantom with EEG cap (PC), for 12-channel rx-only coil, for both cables.

	P_{32} vs. PC_{32}	**P_{64} vs. PC_{64}**	**P_{128} vs. PC_{128}**
p – value (one tail) (Cu cable)	3.51E-11	0.0018	7.47E-08
p – value (two tail) (Cu cable)	7.02E-11	0.0037	1.49E-07
p – value (one tail) (C-fiber cable)	3.58E-08	0.0593	2.79E-04
p – value (two tail) (C-fiber cable)	7.15E-08	0.1187	5.57E-04

Upon performing pair-wise t – tests amongst different density EEG caps (average SNR values obtained for five ROIs from three slices, for one density EEG

array) for the two different EEG cables, it was found that SNR drops as the EEG array density is increased from 32 to 64. But from 32 to 128, the SNR drop is not significant for either of the two sets of cables, as is shown in Table 4.4. The difference between the SNR for 64 - and 128 – channel EEG caps was found to be insignificant and the SNR was found to be higher for 128 – channel EEG cap scan than for the 64 – channel EEG cap scan.

Table 4.4 Results of pair-wise t-test between SNR of phantom with EEG cap (**PC**) condition for when copper - cable was used and when carbon – fiber cable was used across all three EEG array densities, for 12-channel receive only coil.

	PC_{32} vs. PC_{64}	**PC_{64} vs. PC_{128}**	**P_{32} vs. PC_{128}**
p – value (one tail) Cu cable	1.28E-05	0.01	0.09
p – value (one tail) C – fiber cable	3.14E-04	4.33E-04	0.39

4.1.2 Transmit - Receive Coil

The comparative absolute and normalized SNR (SNR with electrode cap divided by SNR without electrode cap) values for all three EEG array densities for the phantom with EEG cap with copper - cable using the transmit-receive coil are shown below in Figures 4.7 and 4.8.

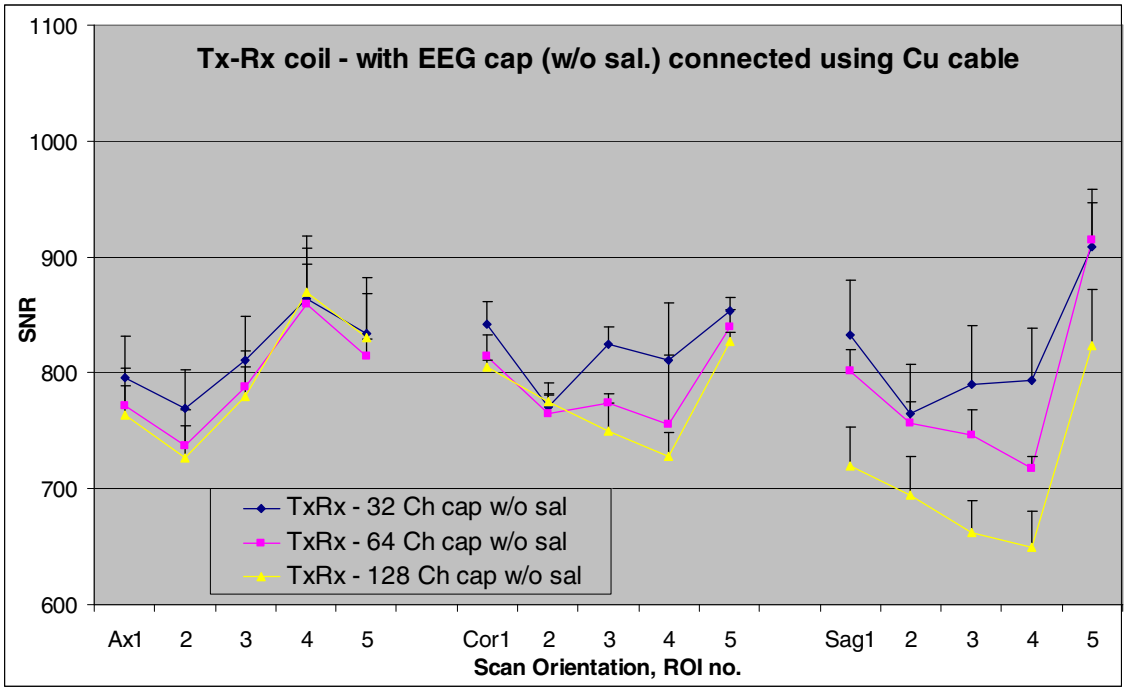

Figure 4.7 Comparison of absolute SNR for all 3 EEG electrode density caps for the transmit-receive head coil, when copper - cable was used.

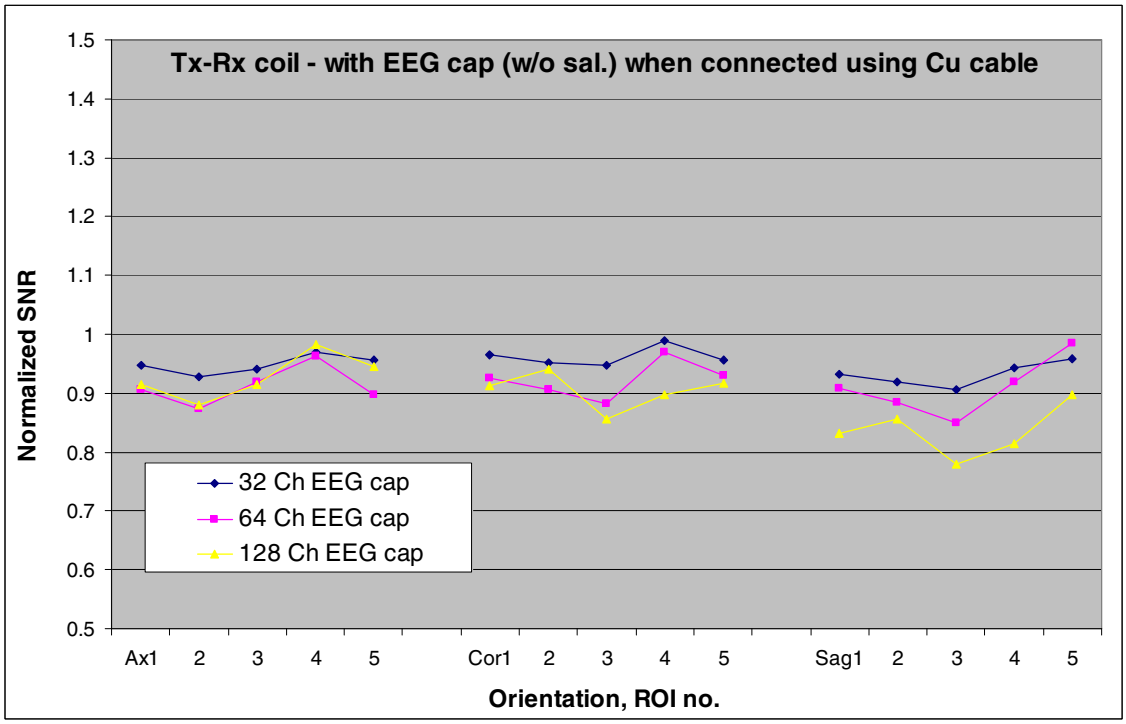

Figure 4.8 Comparison of normalized SNR for all 3 EEG electrode density caps for the transmit-receive head coil, when copper - cable was used.

The plots in Figures 4.9 and 4.10 below depict the absolute and normalized SNR (SNR with electrode cap divided by SNR without electrode cap) respectively, for the 12-channel receive-only head coil when the EEG cap is on the phantom and the carbon fiber cable was used to connect the caps to the head-box (amplifier). It can be seen from Fig. 4.8 that the normalized SNR for the phantom with EEG cap condition was consistently less than 1 for all three EEG array densities and across all orientations. This result is along expected lines unlike the results for 12 – channel receive – only coil

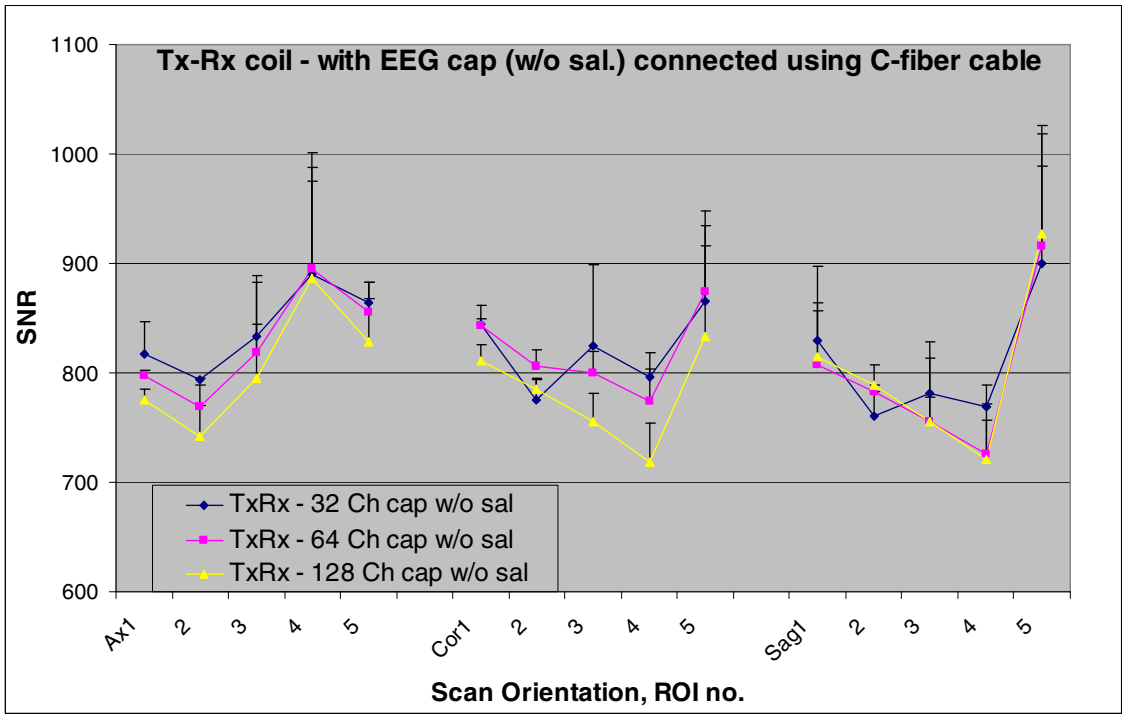

Figure 4.9 Comparison of absolute SNR for all 3 EEG electrode density caps for the transmit-receive head coil, when carbon - fiber cable was used.

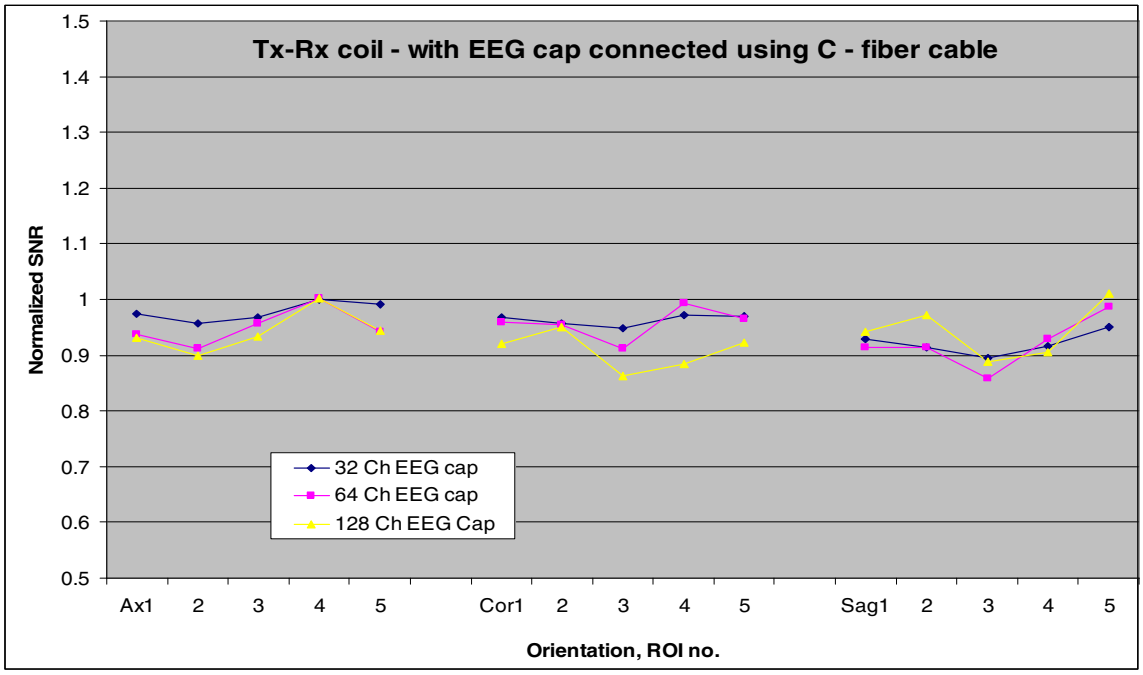

Figure 4.10 Comparison of normalized SNR for all 3 EEG electrode density caps for the transmit - receive head coil, when carbon - fiber cable was used.

Table 4.5 shows p-values for the transmit-receive coil SNR data for the comparison of SNR with EEG cap to without EEG cap, for the three EEG caps and two types of cables. It was found that the SNR goes down significantly (according to the corrected alpha of 0.005) in all the cases (all EEG caps connected using either EEG cable), as is shown in Table 4.5 on the next page.

Table 4.5 Results of pair-wise t-test between SNR of phantom (P) and SNR of phantom with EEG cap (PC), for transmit-receive coil, for both cables.

	P_{32} vs. PC_{32}	**P_{64} vs. PC_{64}**	**P_{128} vs. PC_{128}**
p – value (one tail) (Cu cable)	5.02E-08	2.1E-07	5.84E-07
p – value (two tail) (Cu cable)	1E-07	4.2E-07	1.17E-06
p – value (one tail) (C-fiber cable)	1.42E-05	2.27E-05	8.8E-06
p – value (two tail) (C-fiber cable)	2.84E-05	4.53E-05	1.76E-05

Table 4.6 shows that for the transmit-receive coil, SNR between different scans with different density EEG caps on the phantom, varies significantly with the number of EEG electrodes on the cap

Table 4.6 Results of pair-wise t-test between SNR of phantom with EEG cap (**PC**) condition for when copper - cable was used and when carbon – fiber cable was used across all three EEG array densities, for transmit – receive coil.

	PC_{32} vs. PC_{64}	**PC_{64} vs. PC_{128}**	**P_{32} vs. PC_{128}**
p – value (one tail) Cu cable	0.0001	0.0035	0.0002
p – value (one tail) C – fiber cable	0.0699	0.0014	0.0022

Based on reference [8], it was hypothesized that the SNR of the images would drop with increasing density of EEG electrodes on the EEG cap. But the results shown in Figures 4.3 thru 4.10 fail to corroborate that fully. The transmit-receive coil exhibits this behavior, especially for the sagittal slice orientation with the copper - cable. For the 12-channel receive-only coil, the phantom with the 64-electrode cap consistently

demonstrates lower SNR than with the 32-electrode and 128-electrode caps, and there is no consistent difference between SNR for the 32- and 128-electrode cap situations. For a few orientations and ROIs, the SNR with the 128-electrode cap is higher than with the 32-electrode cap. In other words, the interaction between the head coil elements and the EEG electrodes on the cap, might be enhancing the SNR of the MR signal from the phantom in a few instances.

4.2 Carbon - fiber Cable vs. Copper - cable

The different cables available in the lab (carbon - fiber cable and copper - cable) were used to connect the EEG cap to the head box and were tested for their effect on the MR image SNR when the EEG acquisition system is active (ON).

Figures 4.11 thru 4.13 depict the comparison plots of normalized SNR (SNR with electrode cap divided by SNR without electrode cap) for 32 - , 64 - , and 128 – channel EEG arrays, when carbon – fiber as well as copper - cables were used to connect the caps to the amplifiers and when the scanning was done using the 12-channel rx – only coil, with added saline in the EEG Quick Cells.

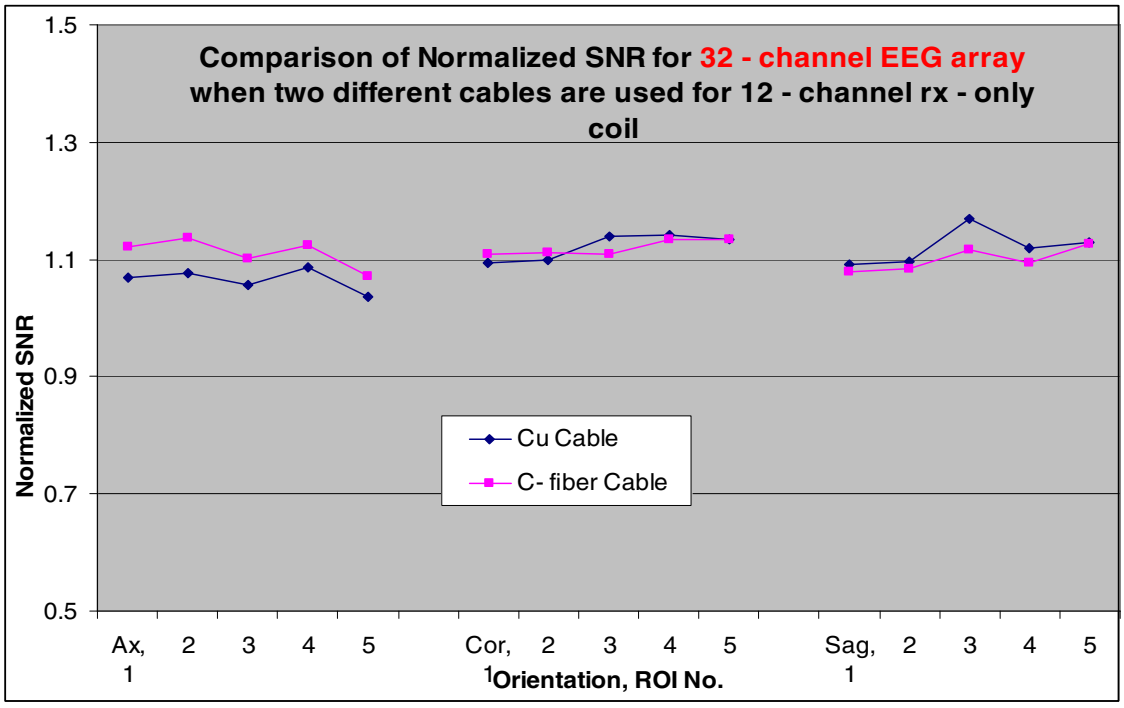

Figure 4.11 Comparison of Normalized SNR for 32 – channel EEG cap (without saline) when both the cables were used for scanning with 12 – channel rx – only coil.

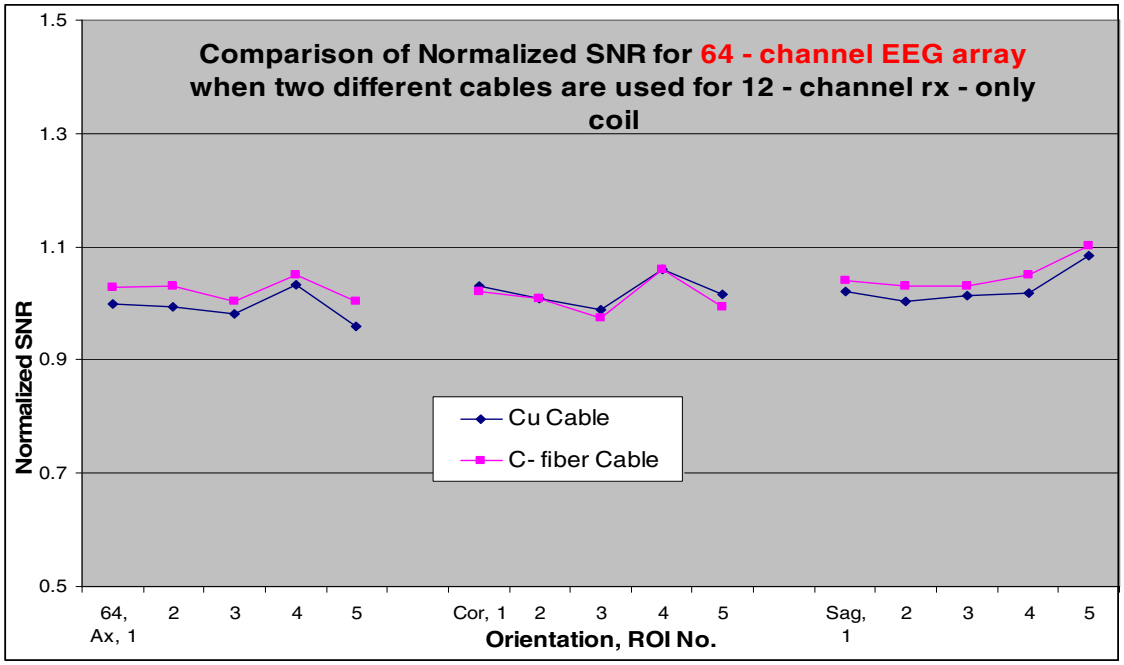

Figure 4.12 Comparison of Normalized SNR for 64 – channel EEG cap (without saline) when both the cables were used for scanning with 12 – channel rx – only coil.

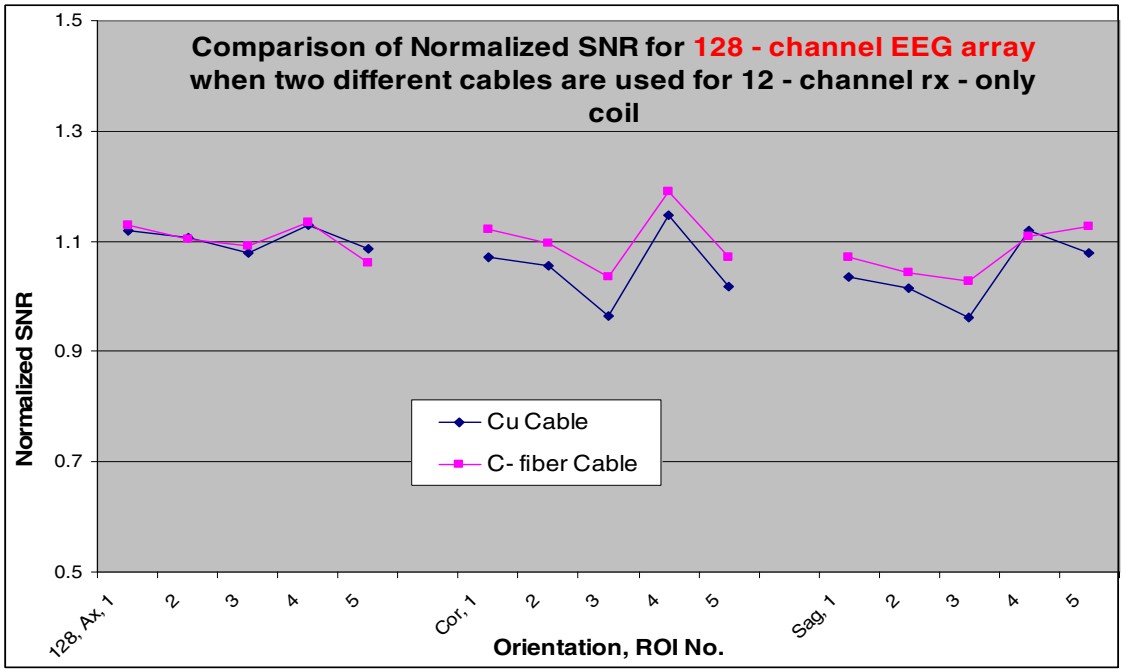

Figure 4.13 Comparison of Normalized SNR for 128 – channel EEG cap (without saline) when both the cables were used for scanning with 12 – channel rx – only coil.

While it was expected that the SNR of the MR images would drop more when EEG cap is connected to amplifier via a carbon - fiber cable than when the cap is connected with the amplifier using a copper - cable, a trend towards the opposite behavior was found for the 12-channel receive-only coil, as tested for significance using pair-wise t-test. The pair – wise t-tests were performed between the fifteen (five ROIs x three slices) SNR data points for a scan across the two conditions. For the 12-channel receive only coil, it was found that there was better SNR with the carbon-fiber cable than with the copper - cable for 64- and 128-channel EEG caps, but no significant difference in SNR was found for the 32-channel EEG cap. The 32-channel EEG cap apparently does not have enough electrodes and associated leads etc. to impact the SNR significantly. From Fig. 4.13 and Table 4.7 it appears that the carbon-fiber

cable performed significantly better than the copper - cable for the 128 channel EEG cap, but the type of cable had no significant impact for the 32 – or 64 – channel EEG cap. But one point to be noted while making this conclusion is that there was no active source (e.g. human head) of electrical activity present during these experimental sessions. Thus, RF interference because of EEG electrodes acting as antennae was minimal.

Table 4.7 Results of pair-wise t-test between SNR of phantom with EEG cap condition for when copper - cable was used ($\mathbf{PC_{N,Cu}}$) and when carbon – fiber cable was used ($\mathbf{PC_{N,C\text{-}f}}$) across all three EEG array densities, with saline, for 12-channel rx - only coil.

	$\mathbf{PC_{32,Cu}}$ **vs.** $\mathbf{PC_{32,C\text{-}f}}$	$\mathbf{P_{64,Cu}}$ **vs.** $\mathbf{PC_{64,C\text{-}f}}$	$\mathbf{P_{128,Cu}}$ **vs.** $\mathbf{PC_{128,C\text{-}f}}$
p – value (one tail)	0.1906	0.0062	0.0009
p – value (two tail)	0.3812	0.0123	0.0017

Figures 4.14 thru 4.16 show graphs of normalized SNR (SNR with electrode cap divided by SNR without electrode cap) for all three EEG array densities when two different cables were used to connect the EEG cap to the amplifiers and when transmit – receive coil was used for scanning, with added saline in the Quick Cells.

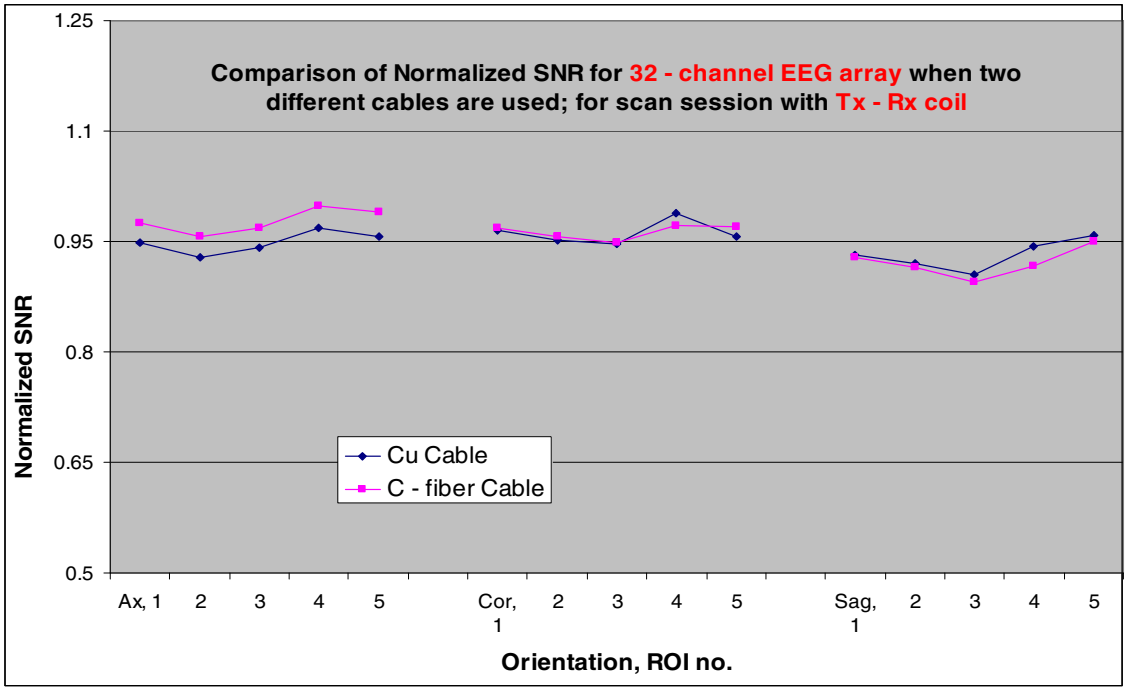

Figure 4.14 Comparison of Normalized SNR for 32 – channel EEG array when two different cables are used to connect the EEG cap (without saline) to the amplifier; for the scanning session with transmit – receive coil.

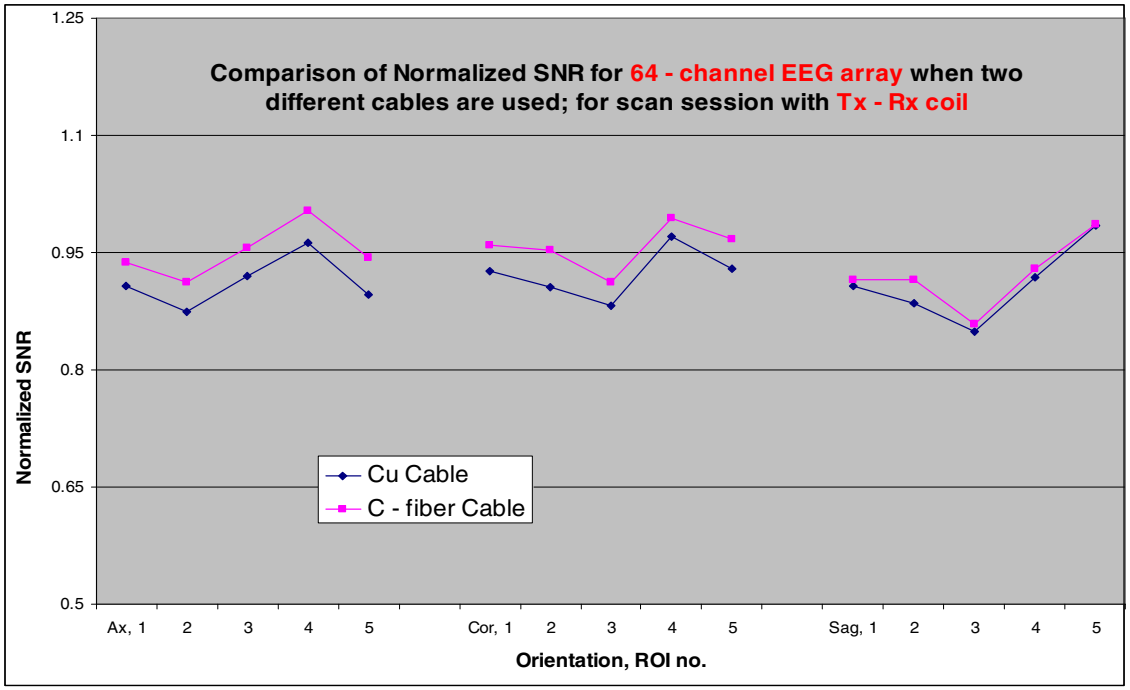

Figure 4.15 Comparison of Normalized SNR for 64 – channel EEG array when two different cables are used to connect the EEG cap (without saline) to the amplifier; for the scanning session with transmit – receive coil.

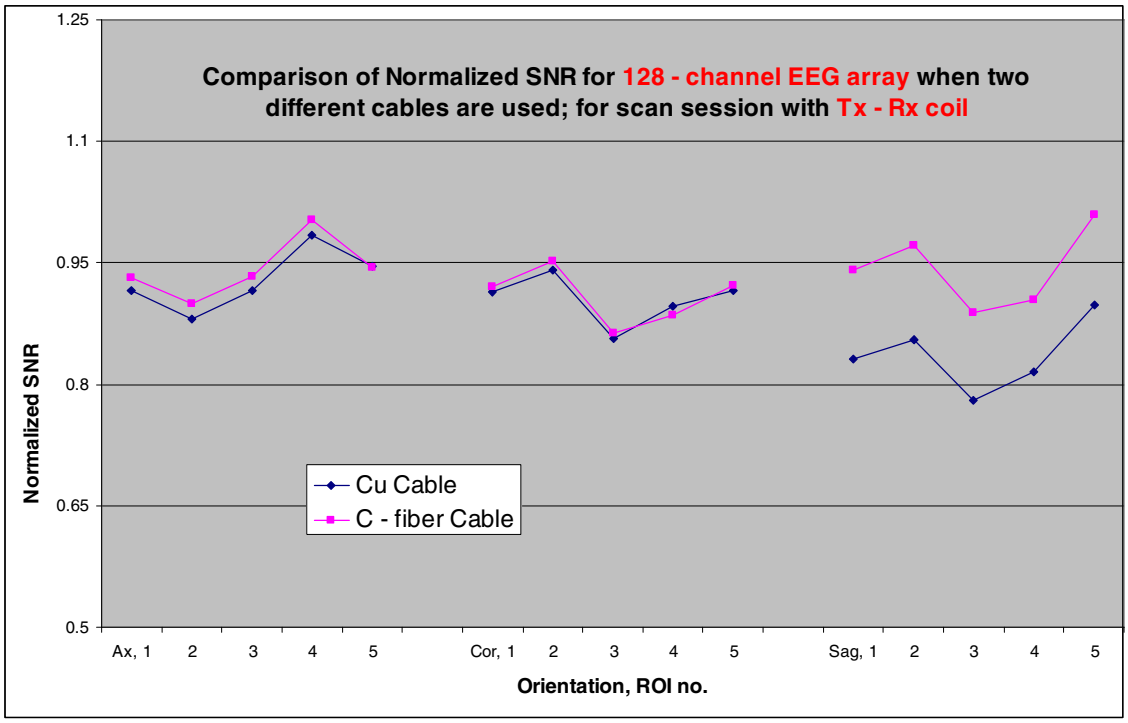

Figure 4.16 Comparison of Normalized SNR for 128 – channel EEG array when two different cables are used to connect the EEG cap (without saline) to the amplifier; for the scanning session with transmit – receive coil.

The carbon – fiber cable seems to impact the SNR for the phantom with EEG cap condition consistently less than when copper - cable is used to connect the EEG caps to the amplifiers.

The results for the paired t-test for transmit-receive coil showed a trend similar to the 12-channel rx-only coil. The difference between SNR was significant for the 64 – and 128 -channel caps for the two different cables but it was not significant for 32-channel EEG cap, as shown in Table 4.8 below. However, the graphs in Figure 4.16 suggest that much of the difference in the 128-electrode case results from the sagittal image orientation; the coronal and axial differences are much smaller.

Table 4.8 Results of pair-wise t-test between SNR of phantom with EEG cap condition, with saline, for when copper - cable was used ($\mathbf{PC_{N,Cu}}$) and when carbon - fiber cable was used ($\mathbf{PC_{N,C\text{-}f}}$) across all three EEG array densities (N) for transmit-receive coil.

	$\mathbf{PC_{32,Cu}}$ **vs.** $\mathbf{PC_{32,C\text{-}f}}$	$\mathbf{P_{64,Cu}}$ **vs.** $\mathbf{PC_{64,C\text{-}f}}$	$\mathbf{P_{128,Cu}}$ **vs.** $\mathbf{PC_{128,C\text{-}f}}$
p – value (one tail)	0.1063	1.92E-06	0.0027
p – value (two tail)	0.2126	3.84E-06	0.0054

4.3 Impact of Using Two Different Head Coils

Fig. 4.17 below shows the plots of normalized SNR obtained from both the head coils in the same chart, when the scans were done with EEG cap (without saline) on the phantom and when the copper - cable was used to connect the EEG caps to the amplifier(s). The three different color lines – blue, pink and yellow represent the three different EEG array densities – 32, 64 and 128, respectively. The solid lines depict the normalized SNR data points for the scans done with the transmit – receive coil and the dotted lines depict the data points for the scans done with the 12 – channel receive – only coil.

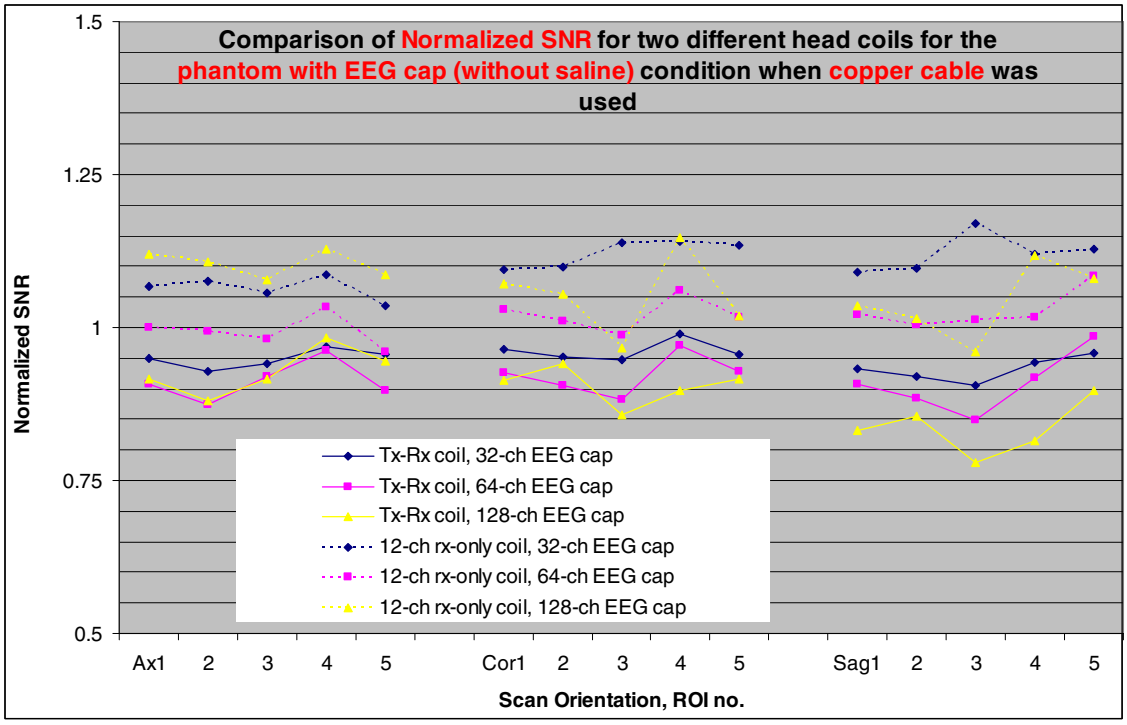

Figure 4.17 Comparison of normalized SNR for phantom with EEG cap condition (without saline) for all three EEG array densities when the scan was done with two different head coils and the EEG caps were connected to amplifiers using the copper - cable.

A pair-wise t-test was performed on the three-slice average normalized SNR for all five ROIs in all three orientations for the scans with the 12-channel receive coil compared to the transmit – receive coil for all three EEG array densities and both the cables. Table 4.9 shows the p-values obtained for a pair-wise t-test between the ROI SNR values for the phantom-only scan (P) and phantom with EEG cap without saline (PC) scan (e.g. P_{32} vs. PC_{32} , P_{64} vs. PC_{64} , P_{128} vs. PC_{128}).

Table 4.9 Results of pair-wise t-test between SNR of phantom (P) and SNR of phantom with EEG cap (PC), for both head coils, for both cables, and all EEG array densities.

	P_{32} vs. PC_{32}	**P_{64} vs. PC_{64}**	**P_{128} vs. PC_{128}**
p – value (one tail) (Cu cable, 12 – Ch rx - only)	3.51E-11	0.0018	7.47E-08
p – value (one tail) (Cu cable, Tx – Rx coil)	5.02E-08	2.1E-07	5.84E-07

While Table 4.9 tells us that the SNR for the phantom with EEG cap condition was significantly different from the SNR for the phantom only scans for both the head coils, the Fig. 4.17 informs us that the SNR was > 1 for the scans done with 12 – channel receive – only coil and it was < 1 for the scans performed with the transmit – receive coil.

Fig. 4.18 below shows the plots of normalized SNR obtained from both the head coils in the same chart, when the scans were done with EEG cap (without saline) on the phantom and when the carbon – fiber cable was used to connect the EEG caps to the amplifier(s). The three different color lines – blue, pink and yellow represent the three different EEG array densities – 32, 64 and 128, respectively. The solid lines depict the normalized SNR data points for the scans done with the transmit – receive coil and the dotted lines depict the data points for the scans done with the 12 – channel receive – only coil.

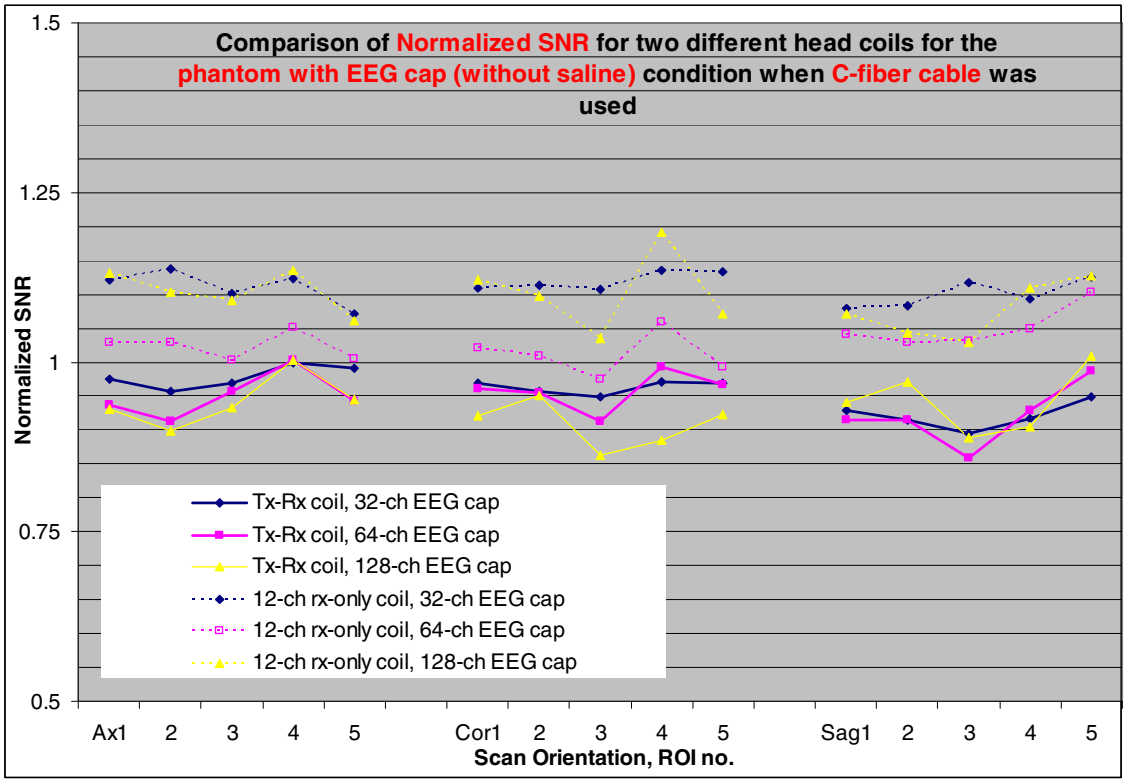

Figure 4.18 Comparison of normalized SNR for phantom with EEG cap condition (without saline) for all three EEG array densities when the scan was done with two different head coils and the EEG caps were connected to amplifiers using the carbon - fiber cable.

Table 4.10 below shows the p-values obtained for a pair-wise t-test between the ROI SNR values for the phantom-only scan (P) and phantom with EEG cap without saline (PC) scan (e.g. P_{32} vs. PC_{32} , P_{64} vs. PC_{64} , P_{128} vs. PC_{128}).

Table 4.10 Results of pair-wise t-test between SNR of phantom (P) and SNR of phantom with EEG cap (PC), for both head coils, for carbon – fiber cables, and all EEG array densities.

	P_{32} vs. PC_{32}	**P_{64} vs. PC_{64}**	**P_{128} vs. PC_{128}**
p – value (one tail) (C-fiber cable, 12 – Ch rx – only)	3.58E-08	0.0593	2.79E-04
p – value (one tail) (C-fiber cable, Tx – Rx coil)	2.84E-05	4.53E-05	1.76E-05

Again, while Table 4.10 tells us that the SNR for the phantom with EEG cap condition was significantly different from the SNR for the phantom only scans (except for the scans with 64 – channel EEG cap) for both the head coils, the Fig. 4.18 informs us that the SNR was > 1 for the scans done with 12 – channel receive – only coil and it was < 1 for the scans performed with the transmit – receive coil.

It can be surmised from the above plots and tables that the 12 – channel receive – only coil interacts with the EEG electrode cap and its components (electrodes, leads and material) differently than that of the transmit – receive coil. Thus, this reinforces the view that every fMRI facility that plans on doing the simultaneous EEG – fMRI studies, must perform such tests before embarking upon full fledged experiments.

4.4 Effect of Conductive Medium on the MR Image SNR

A t-test was used to test the effect of adding saline to the EEG electrode Quick Cells for the different combinations of rf coils, numbers of electrodes, and cable types. For the 12-channel receive coil, the SNR for phantom with EEG cap condition (PC) and phantom with EEG cap with saline condition (PCS) was found to be significantly different only for the 64-electrode cap with the copper - cable (Table 4.11). For the carbon - fiber cable, adding saline made no difference for the 64-electrode cap but significantly changed the SNR for the 32-electrode and 128-electrode arrays (Table 4.11 below).

Table 4.11 Results of pair-wise t-test between SNR of phantom with EEG cap (PC) and SNR of phantom with EEG cap with saline (PCS), for 12-channel receive coil with both EEG cables.

	PC_{32} vs. PCS_{32}	**PC_{64} vs. PCS_{64}**	**PC_{128} vs. PCS_{128}**
p – value (one tail) (Cu cable)	0.23	4.99E-05	0.08
p – value (two tail) (Cu cable)	0.46	9.97E-05	0.16
p – value (one tail) (C-fiber cable)	1.28E-04	0.18	7.78E-04
p – value (two tail) (C-fiber cable)	2.57E-04	0.36	1.56E-03

Upon significance testing the transmit – receive coil data, using pair-wise t-test, it was found that adding saline to the quick cells in the EEG cap (PCS condition) leads to a significant drop in SNR when compared to the phantom with EEG cap only condition (PC) for the 32-electrode and 128-electrode caps (32 > 128) but not the 64-electrode cap, when the carbon - fiber cable is used, as shown in Table 4.12.

Table 4.12 Results of paired wise t-test between SNR of phantom with EEG cap (PC) and SNR of phantom with EEG cap with saline (PCS), for transmit-receive coil with both the EEG cables.

	PC_{32} vs. PCS_{32}	**PC_{64} vs. PCS_{64}**	**PC_{128} vs. PCS_{128}**
p – value (one tail) (Cu cable)	4.62E-07	0.21	4.14E-04
p – value (two tail) (Cu cable)	9.24E-07	0.41	8.27E-04
p – value (one tail) (C-fiber cable)	9.69E-06	2.71E-03	0.48
p – value (two tail) (C-fiber cable)	1.94E-05	5.41E-03	0.96

With copper - cable connecting the EEG cap to the amplifier outside the scanner room, the 32- and 64-electrode caps show decreased SNR with added saline condition (32 > 64), whereas the 128-electrode cap is not affected by adding saline.

4.5 Scarff et.al. 2004[8] vs. This Project

In the Scarff et.al. 2004, the reference which has been repeatedly cited by this project, there is no mention of the head coil that was used for image acquisition. But, as shown in Fig.1.1 earlier, that study has depicted a drop in SNR when the density of EEG array was increased from 64 to 128 and subsequently to 256 electrodes. The experiments were performed at 3T on human subjects with an EPI sequence and oblique axial slices, and the ROI for signal measurement was placed in the white matter.

Similar plots with SNR values obtained from centrally placed ROI (ROI 1) in axial, coronal and sagittal scans were prepared for both the head coils as shown in figures below. The normalized SNR values for Scarff et.al. study were approximated from Fig. 1.1 in the paper and were plotted along with the normalized SNR values from this study's scans for both the head coils but only for the scans which were performed when carbon-fiber cable was used to connect the EEG electrode caps to the amplifiers, as shown in Figures 4.19, 4.21 and 4.23 further ahead in this section. This was done in order to do useful comparison by keeping the conditions similar to those of Scarff et al. These plots do not completely corroborate the drop in SNR seen by Scarff et.al. study.

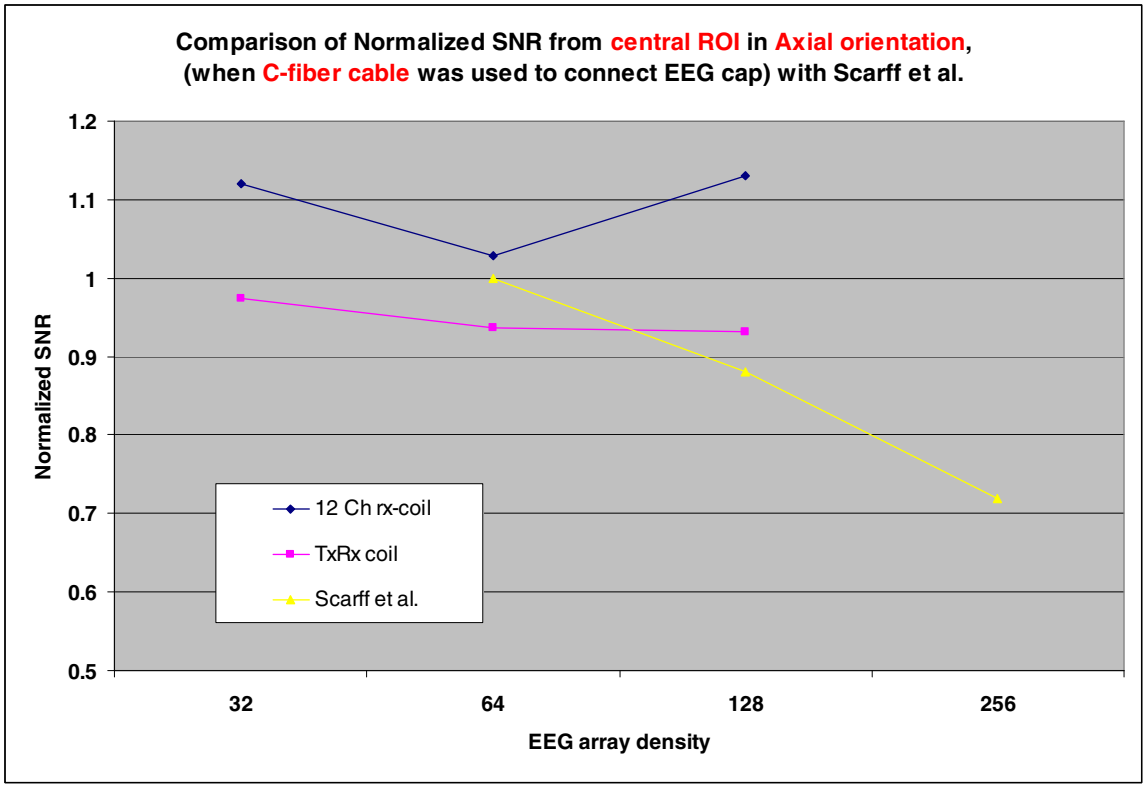

Figure 4.19 Comparison of normalized SNR from central ROI, axially oriented scans in this project (for both head coils, for carbon - fiber cable) with approx. values from Scarff et.al.

Fig.4.20 below is a similar comparison of SNR between this study and Scarff et al. study when copper - cable was used.

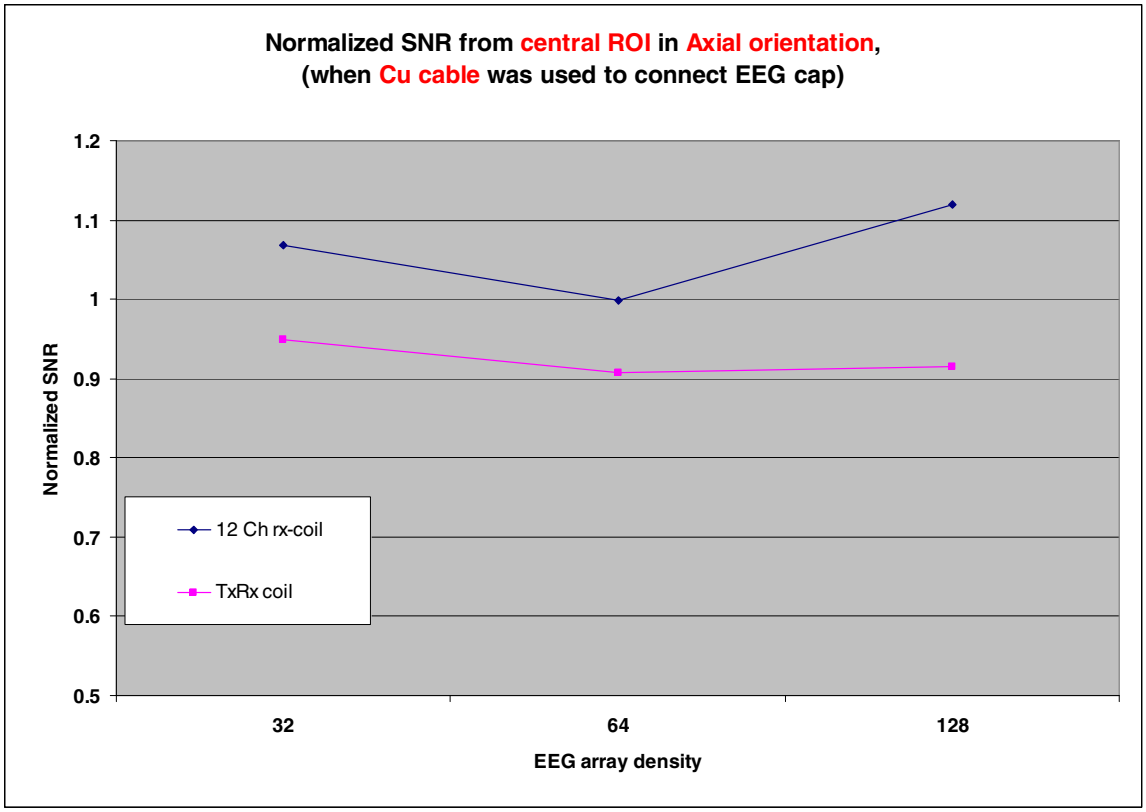

Figure 4.20 Comparison of normalized SNR from central ROI, axially oriented scans in this project (for both head coils, for copper - cable).

Figures 4.21 and 4.22 below compare the SNR for coronally oriented scans obtained from both the head coils when carbon - fiber and copper - cables were used respectively.

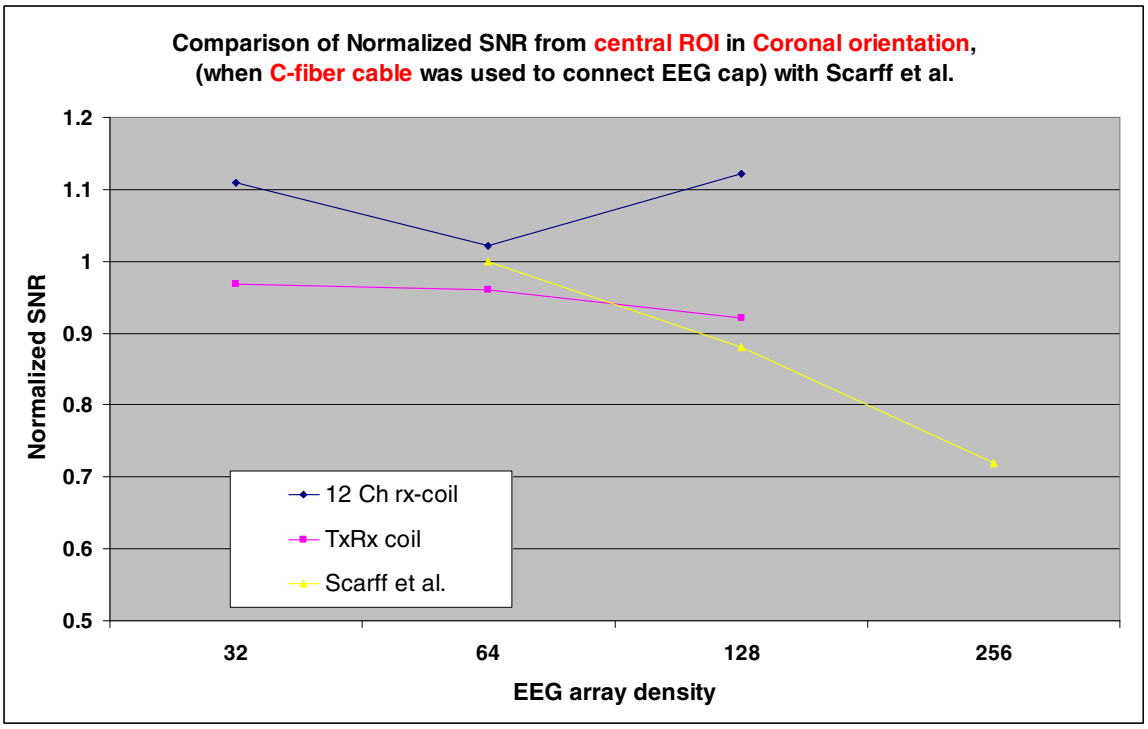

Figure 4.21 Comparison of normalized SNR from central ROI, coronally oriented scans in this project (for both head coils, for carbon - fiber cable) with approx. values from Scarff et.al.

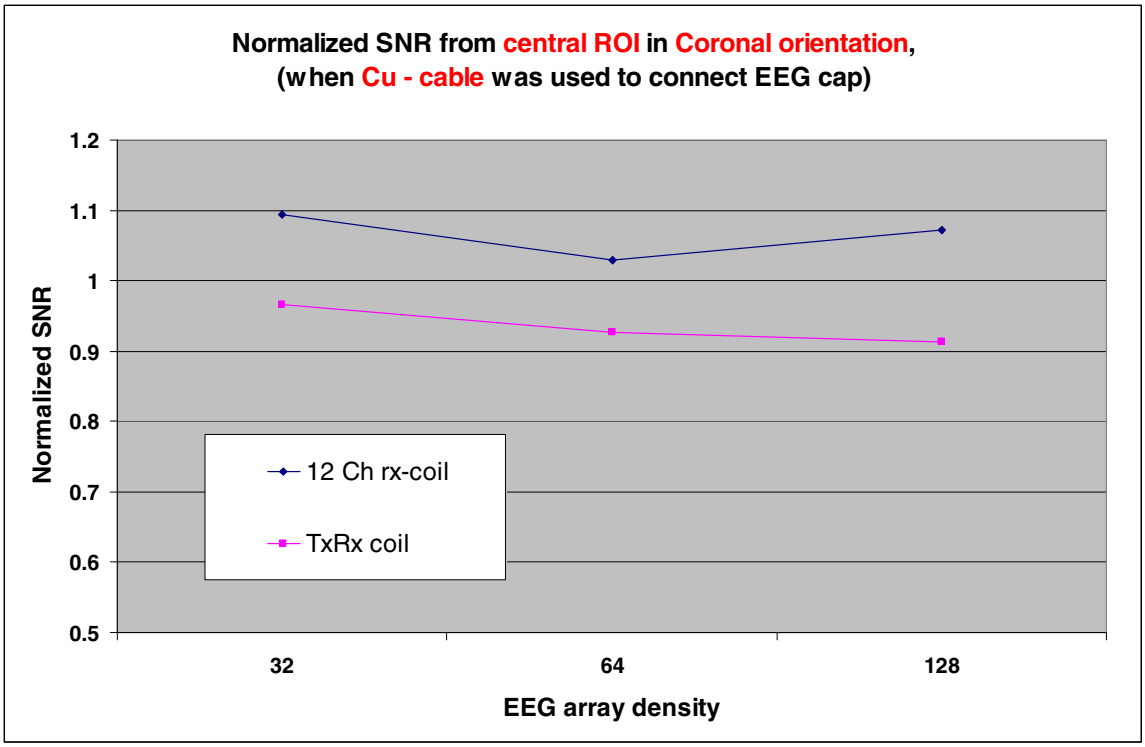

Figure 4.22. Comparison of normalized SNR from central ROI, coronally oriented scans in this project (for both head coils, for copper - cable)

Figures 4.23 and 4.24 compare the SNR for sagittally oriented scans obtained from both the head coils when carbon - fiber and copper - cables were used respectively.

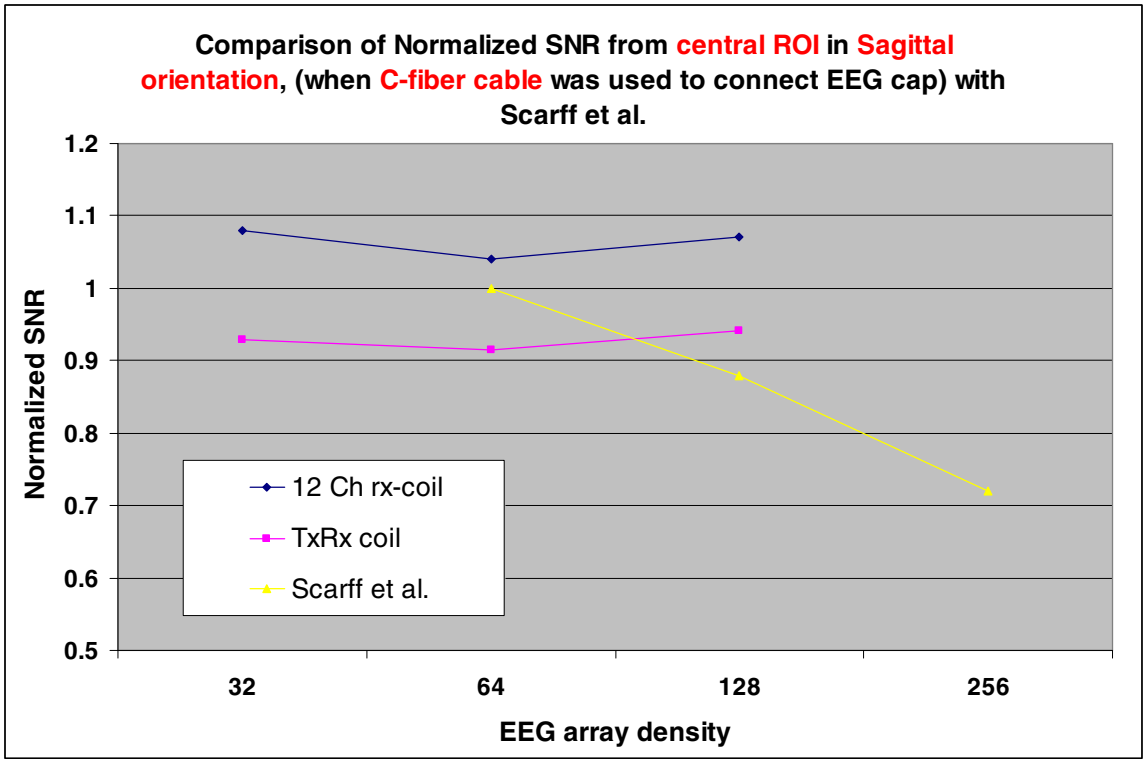

Figure 4.23 Comparison of normalized SNR from central ROI, sagittally oriented scans in this project (for both head coils, for carbon - fiber cable) with approx. values from Scarff et.al.

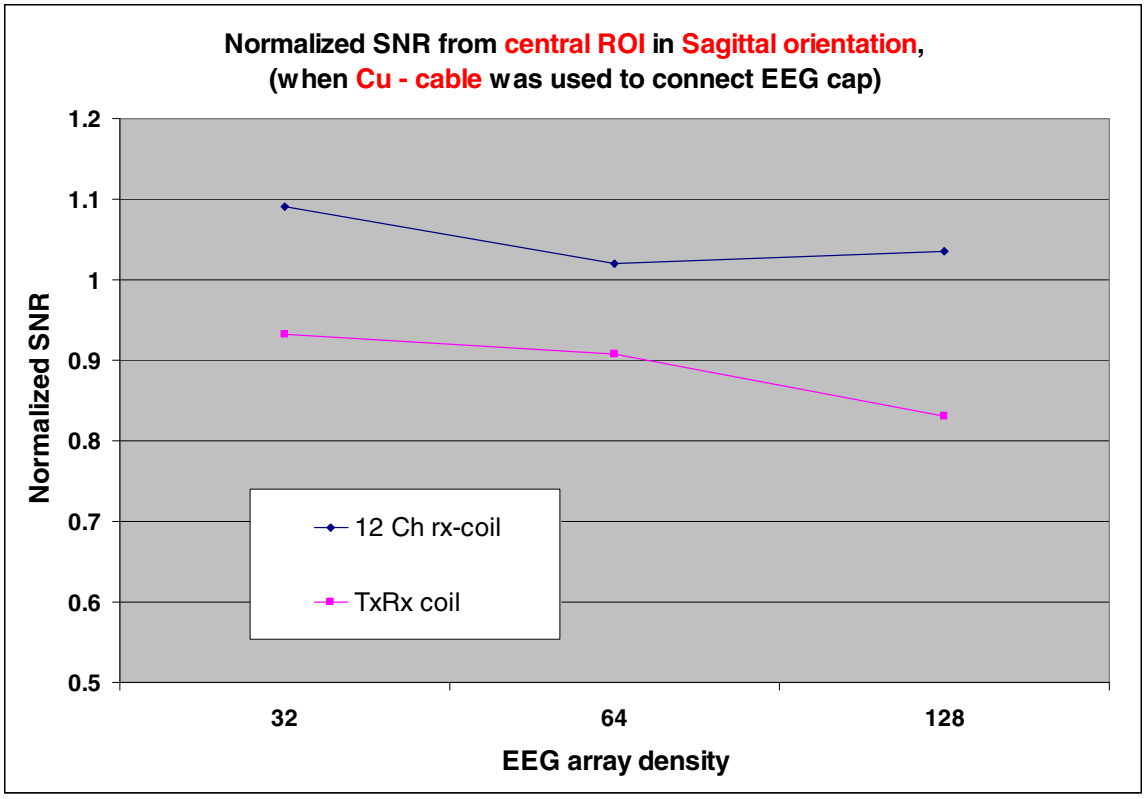

Figure 4.24 Comparison of normalized SNR from central ROI,sagittally oriented scans in this project (for both head coils, for copper - cable)

The only set of scans where the SNR seems to follow a pattern according to the findings of Scarff et.al. paper are when sagittally oriented scans were acquired for the phantom with 64- and 128-electrode cap condition with transmit-receive head coil and two kinds of EEG cables. Interestingly, the 32-electrode cap shows a decreased SNR even as compared to 64-electrode cap.

The normalized SNR for all the scans with the 12-channel receive coil had values > 1. This implies that something contributed to the signal when the scans were performed with EEG cap on the phantom. M. D. Schnall et al [13] and E. D. Wirth et al. [14] reported seeing an increase in the SNR of the spinal cord region when they placed an inductively couple coil close to the original receiver coil. This phenomenon might

also help explain the increase in SNR in the case of scans performed with 12-channel receive –only coil when EEG cap was on the phantom because, the EEG electrodes might act as auxiliary surface coils which get inductively coupled with the elements of the head coil. The transmit-receive coil does not suffer from these effects as it has a bigger separation between the phantom (and the electrodes on it) and the coil elements. Further investigation to confirm this is definitely warranted.

The comparisons of our data with the Scarff et al. paper done in Figures 4.19, 4.21 and 4.23 suffer from not having exactly identical conditions because this study:

1. Used silicone oil phantom instead of an actual human subject.
2. Used 32-, 64-, and 128-channel EEG electrode arrays instead of 64, 128 and 256.
3. Used axially, coronally and sagittally oriented scans, while the Scarff et.al. paper used an oblique axial orientation.
4. Used centrally placed ROI while Scarff et.al. used ROI s placed in white matter.
5. Used a 12-channel receive as well as transmit-receive coil while Scarff et.al. paper didn't mention the coil used.
6. Used a gradient echo 2-D FLASH sequence while the Scarff et al. study used a gradient echo EPI sequence.
7. Used copper - cable as well as carbon - fiber cable to connect EEG caps to the amplifier while Scarff et.al. used carbon - fiber cable only.

CHAPTER 5

CONCLUSION

This study examined the effect of number of EEG electrodes, type of head coil, type of cable (copper or carbon - fiber conductor), presence or absence of added saline in the Neuroscan MagLink Quick Cells, and slice orientation on the MRI SNR in five different locations in a phantom.

The expected drop in the SNR of the images because of the increased density of the EEG electrode array is not so straightforward as was made out to be in Scarff et, al., 2004 [8], While they found a linear drop in SNR as depicted in Fig.1 cited in section 1.3 of this thesis, this study found that the drop in SNR is not as apparent. The head coil and sample (phantom or head) being used, the scan orientation, and the number of EEG electrodes are all factors that govern the quality of the MR images obtained during simultaneous EEG-fMRI. The trend for decreased SNR with increased number of electrodes was observed for the transmit-receive coil but not for the 12-channel coil.

Significant variation was noticed in the SNR vis a vis the positioning of signal ROIs in the FOV for the 12-channel receive-only array coil. For the 12-channel array coil, the ROIs closer to the periphery of the phantom had an improved SNR as compared to the ROI placed at the center of the phantom. The SNR also varied for different scan orientations – axial, coronal and sagittal.

Significant dependence on saline was noticed for some of the coil-cable-electrode combinations as indicated in Tables 4.10 and 4.11.

For both the the 12-channel receive-only coil and the transmit-receive coil, the carbon - fiber cable seemed to performed better than the copper - cable for the 64 as well as 128 channel EEG cap, but the type of cable had no significant impact for the 32-electrode EEG cap.

The largest, most obvious, and most consistent effect noted was that while EEG electrodes produced the expected reduction in SNR for the transmit-receive coil, EEG electrodes increased SNR for the 12-channel receive-only array head coil.

CHAPTER 6

FUTURE WORK

It was the goal of this study to try to fill in some blanks in the sparse and spotty literature available on this topic. Though a concerted effort was made in that direction, the work is far from complete.

The very next step is to perform these experiments on a human head so that data for these important experimental conditions can be obtained. As all BOLD fMRI studies use an EPI (echo planar imaging) sequence for imaging the brain, a set of experiments using EPI sequence with human subjects is needed. It is also intended to perform similar experiments for an EEG cap with 256 electrodes when it becomes available to us, thereby allowing us to add another data point to the plot of SNR dependence upon the density of EEG electrode arrays.

To get a convincing answer to the questions posed by this study, more than one measurement is required for all the independent variables. Then it will also be possible to perform multivariate analysis based on different variables.

REFERENCES

1. Logothetis, N. K., Pauls, J., Augath, M., Trinath, T., and Oeltermann, A. (2001). Neurophysiological investigation of the basis of the fMRI signal. Nature 412, 150–157.

2. Logothetis, N. K., and Pfeuffer, J. (2004). On the nature of the BOLD fMRI contrast mechanism. Magn. Reson. Imaging 22, 1517–1531.

3. Garreffa G, Bianciardi M, Hagberg GE, Macaluso E, Marciani MG, Maraviglia B, Abbafati M, Carni M, Bruni I, Bianchi L. Simultaneous EEG-fMRI acquisition: how far is it from being a standardized technique? Magn Reson Imaging. 2004 Dec;22(10):1445-55.

4. Neuroscan Product Notes – manual 7228C, Neuroscan, El Paso, Texas.

5. Baumann SB, Noll DC. A modified electrode cap for EEG recordings in MRI scanners. Clin Neurophysiol. 1999 Dec;110(12):2189-93.

6. Krakow K, Allen PJ, Symms MR, Lemieux L, Josephs O, Fish DR. EEG recording during fMRI experiments: image quality. Hum Brain Mapp. 2000 May;10(1):10-5.

7. Bonmassar G, Hadjikhani N, Ives JR, Hinton D, Belliveau JW. Influence of EEG electrodes on the BOLD fMRI signal. Hum Brain Mapp. 2001 Oct;14(2):108-15.

8. Scarff CJ, Reynolds A, Goodyear BG, Ponton CW, Dort JC, Eggermont JJ. Simultaneous 3-T fMRI and high-density recording of human auditory evoked potentials. Neuroimage. 2004 Nov;23(3):1129-42.

9. Iannetti GD, Niazy RK, Wise RG, Jezzard P, Brooks JC, Zambreanu L, Vennart W, Matthews PM, Tracey I. Simultaneous recording of laser-evoked brain potentials and continuous, high-field functional magnetic resonance imaging in humans. Neuroimage. 2005 Nov 15;28(3):708-19.

10. Neuroscan Product Notes - Maglink manual 7290A, Neuroscan, El Paso, Texas.

11. Collins CM, Liu W, Schreiber W, Yang QX, Smith MB. Central brightening due to constructive interference with, without, and despite dielectric resonance. J Magn Reson Imaging. 2005 Feb;21(2):192-6.

12. Yang QX, Mao W, Wang J, Smith MB, Lei H, Zhang X, Ugurbil K, Chen W. Manipulation of image intensity distribution at 7.0 T: passive RF shimming and focusing with dielectric materials. J Magn Reson Imaging. 2006 Jul;24(1):197-202.

13. Schnall MD, Barlow C, Subramanian VH, Leigh JS Jr. Wireless Implanted magnetic Resonance probes for in Vivo NMR. J Magn Reson. 1986;161-167.

14. Wirth ED, Mareci TH, Beck BL, Fitzsimmons JR, Reier PJ. A comparison of an inductively coupled implanted coil with optimized surface coils for in vivo NMR imaging of the spinal cord. Magn. Reson. in Med. 1993 Nov;30(5):626-640.

BIOGRAPHICAL INFORMATION

Aman Ish Goyal earned a B.Tech (Bachelor in Technology) degree in Electronics and Communication Engineering from Punjab Technical University, India in 2003. He joined the joint program of Biomedical Engineering between University of Texas at Arlington and University of Texas Southwestern Medical Center at Dallas in the spring of 2004. Since the summer of 2005 he has worked at the Gulf War Syndrome - Neuroimaging lab under the aegis of Dr. Richard W. Briggs as a graduate student research assistant. He graduated with an MS degree in Biomedical Engineering in December 2006.